J Physiol 589.23 (2011) pp 5857–5878

The Journal of Physiology

The *GABRA6* mutation, *R46W*, associated with childhood absence epilepsy, alters $\alpha6\beta2\gamma2$ and $\alpha6\beta2\delta$ $GABA_A$ receptor channel gating and expression

Ciria C. Hernandez[1], Katharine N. Gurba[4], Ningning Hu[1] and Robert L. Macdonald[1,2,3]

Departments of [1]Neurology, [2]Molecular Physiology and Biophysics, and [3]Pharmacology, and [4]Program in Neuroscience, Vanderbilt University, Nashville, TN 37232, USA

Non-technical summary Childhood absence epilepsy (CAE) is a genetic form of epilepsy that typically develops at 4–8 years of age with brief losses of consciousness and frequent staring spells. Genetic defects or mutations associated with this disorder have been found in specialized membrane proteins called $GABA_A$ receptor channels. $GABA_A$ receptors are ligand-gated chloride channels, and the majority are thought to be composed of α, β and γ or α, β and δ subunit proteins that mediate both rapid, phasic inhibitory synaptic transmission and steady-state, tonic perisynaptic inhibition in the nervous system. Here we showed that a novel $GABA_A$ receptor $\alpha6$ subunit mutation linked with CAE, R46W, impaired gating and assembly of both $\alpha\beta\gamma$ and $\alpha\beta\delta$ $GABA_A$ receptors. These findings suggested that the CAE-associated $\alpha6$(R46W) subunit mutation could cause neuronal disinhibition and thus increase susceptibility to generalized seizures through a reduction of $\alpha\beta\gamma$ and $\alpha\beta\delta$ receptor function and expression.

Abstract A $GABA_A$ receptor $\alpha6$ subunit mutation, R46W, was identified as a susceptibility gene that may contribute to the pathogenesis of childhood absence epilepsy (CAE), but the molecular basis for alteration of $GABA_A$ receptor function is unclear. The R46W mutation is located in a region homologous to a $GABA_A$ receptor $\gamma2$ subunit missense mutation, R82Q, that is associated with CAE and febrile seizures in humans. To determine how this mutation reduces GABAergic inhibition, we expressed wild-type ($\alpha6\beta2\gamma2$L and $\alpha6\beta2\delta$) and mutant ($\alpha6$(R46W)$\beta2\gamma2$L and $\alpha6$(R46W)$\beta2\delta$) receptors in HEK 293T cells and characterize their whole-cell and single-channel currents, and surface and total levels. We demonstrated that gating and assembly of both $\alpha6$(R46W)$\beta2\gamma2$L and $\alpha6$(R46W)$\beta2\delta$ receptors were impaired. Compared to wild-type currents, $\alpha6$(R46W)$\beta2\gamma2$L and $\alpha6$(R46W)$\beta2\delta$ receptors had a reduced current density, $\alpha6$(R46W)$\beta2\gamma2$L currents desensitized to a greater extent and deactivated at a slower rate, $\alpha6$(R46W)$\beta2\delta$ receptors did not desensitize but deactivated faster and both $\alpha6$(R46W)$\beta2\gamma2$L and $\alpha6$(R46W)$\beta2\delta$ single-channel current mean open times and burst durations were reduced. Surface levels of coexpressed $\alpha6$(R46W), $\beta2$ and δ, but not $\gamma2$L, subunits were decreased. 'Heterozygous' coexpression of $\alpha6$(R46W) and $\alpha6$ subunits with $\beta2$ and $\gamma2$L subunits produced intermediate macroscopic current amplitudes by increasing incorporation of wild-type and decreasing incorporation of mutant subunits into receptors trafficked to the surface. Finally, these findings suggest that similar to the $\gamma2$(R82Q) mutation, the CAE-associated $\alpha6$(R46W) mutation could cause neuronal disinhibition and thus increase susceptibility to generalized seizures through a reduction of $\alpha\beta\gamma$ and $\alpha\beta\delta$ receptor function and expression.

(Resubmitted 17 August 2011; accepted 16 September 2011; first published online 19 September 2011)

Corresponding author R. L. Macdonald: Vanderbilt University Medical Center, 6140 Medical Research Building III, 465, 21st Ave, Nashville, TN 37232-8552, USA. Email: robert.macdonald@vanderbilt.edu

Abbreviations AChR, acetylcholine receptor; CAE, childhood absence epilepsy; HEK 293T, human embryonic kidney cells; nAChR, nicotinic acetylcholine receptor; wt, wild-type.

© 2011 The Authors. Journal compilation © 2011 The Physiological Society

DOI: 10.1113/jphysiol.2011.218883

Introduction

$GABA_A$ receptors, the major mediators of inhibition in the mammalian central nervous system, belong to the Cys-loop ion channel superfamily, which includes glycine, nicotinic acetylcholine (nAChR), and serotonin 5-HT_3 receptors. $GABA_A$ receptor subunits have an ∼200 residue N-terminal extracellular domain and four transmembrane segments (M1, M2, M3, M4) that are homologous to the ACh binding protein N-terminal domain (Brejc *et al.* 2001) and the transmembrane domain of the *Torpedo marmorata* ACh receptor (AChR) (Miyazawa *et al.* 2003). $GABA_A$ receptors are formed by pentameric assembly of 19 different subunit subtypes (α1–α6, β1–β3, γ1–γ3, δ, ε, π, θ and ρ1–ρ3), although the majority of receptors are thought to be $\alpha\beta\gamma$ and $\alpha\beta\delta$ receptor isoforms that mediate both phasic inhibitory synaptic transmission and tonic perisynaptic inhibition (Macdonald & Olsen, 1994).

Idiopathic epilepsy syndromes are primarily genetic diseases and are characterized by typical seizure types and EEG abnormalities and are not associated with structural brain lesions (Hirose *et al.* 2005). Mutations or variants associated with idiopathic generalized epilepsies (IGEs) have been associated with $GABA_A$ receptor subunit α1, β3, γ2 and δ genes (*GABRA1*, *GABRB3*, *GABRG2* and *GABRD*, respectively; Macdonald *et al.* 2010). A novel $GABA_A$ receptor α6 subunit mutation, *GABRA6(R46W)*, was recently described in an IGE cohort study in a patient with childhood absence epilepsy (CAE) (Dibbens *et al.* 2009), but no evidence of channel impairment was reported. The mutation is located in a region homologous to that of the $GABA_A$ receptor γ2 subunit mutation, R82Q (R43Q in the mature peptide), which is associated with CAE and febrile seizures in humans (Wallace *et al.* 2001; Marini *et al.* 2003). Mutant γ2(R82Q) subunits reduced both surface $\alpha1\beta2\gamma2$(R82Q) receptor levels (Kang & Macdonald, 2004) and receptor currents (Bianchi *et al.* 2002*b*), suggesting impairment of both assembly and function of $GABA_A$ receptors.

Homology modelling of the N-terminal extracellular domain of human $\beta2\alpha6\beta2\alpha6\gamma2$ and $\beta2\alpha6\beta2\alpha6\delta$ $GABA_A$ receptors suggested that the α6 subunit mutation, R46W (Fig. 1*A* and Fig. 10*C*), is located within a loop (L1) between the α-helix and the β1-sheet (Fig. 1*B*), where it contributes to the α/β, α/γ and α/δ subunit interfaces in assembled receptors. In contrast, the γ2 subunit mutation R82Q (Fig. 1*A*) only contributes to the γ/α interface. Sequence alignment of the ACh binding protein with the α-helix–L1–β1-sheet region of human α6, γ2L, β2 and δ subunits and the *T. marmorata* AChR α1 subunit showed conserved structural relationships (Fig. 1*B*).

To gain further insights into the effects of the R46W mutation on $GABA_A$ receptor function and assembly, we studied the gating properties and surface expression of $\alpha6\beta2\gamma2$, $\alpha6$(R46W)$\beta2\gamma2$, $\alpha6$(R46W)$\beta2\gamma2$, $\alpha6\beta2\delta$ $\alpha6/\alpha6$(R46W)$\beta2\delta$ and $\alpha6$(R46W)$\beta2\delta$ subunits expressed in cells of the human embryonic kidney cell line HEK 293T. We found that the R46W mutation impaired gating and assembly of both $\alpha6$(R46W)$\beta2\gamma2$L and $\alpha6$(R46W)$\beta2\delta$ receptors and substantially reduced the current density of both receptors. In addition, surface levels of coexpressed α6(R46W), β2 and δ subunits, but not γ2L subunits, were decreased. These findings suggested that the CAE-associated α6(R46W) mutation could cause neuronal disinhibition and thus increase susceptibility to generalized seizures through a reduction of $\alpha\beta\gamma$ and $\alpha\beta\delta$ receptor function and expression, sharing a mechanism with the γ2(R82Q) mutation linked with CAE in humans.

Methods

cDNA constructs

cDNAs encoding human α6, β2, γ2L and δ $GABA_A$ receptor subunit subtypes (GenBank accession numbers NM000811, NM000813, NM198904 and NM000815, respectively) were subcloned into the plasmid expression vector pcDNA3.1 (Invitrogen, Carlsbad, CA, USA) using standard techniques. The human α6 subunit mutation, R46W, was generated by site-directed mutagenesis using the QuickChange Site-Directed Mutagenesis Kit (Stratagene, La Jolla, CA, USA) and verified by sequencing. FLAG (DYKDDDDK) or HA (YPYDVPDYA) epitopes were inserted between amino acids 4 and 5 of the mature α6, γ2L and δ subunits, so that subunit total and cell surface expression could be determined by flow cytometry. In this study all mutations were specified in the immature peptide, which has been the convention in the literature for α1, β3 and δ subunit mutations and variants but not for γ2 subunit mutations, which have generally been identified in the mature peptide (Macdonald *et al.* 2010).

Cell culture and transfections

HEK 293T cells were grown in 100 mm tissue culture dishes (Corning) in Dulbecco's modified Eagle's medium (DMEM), supplemented with 10% fetal bovine serum at 37°C in 5% CO_2–95% air. For electrophysiological experiments, cells were plated onto poly-L-lysine-coated (cell-attached and excised outside-out patches) or non-coated (lifted whole cells) coverglass chips and transfected with 0.3 μg of each subunit plasmid in a ratio of $1^{\alpha6}:1^{\beta2}:1^{\gamma2L/\delta}$ (wild-type or homozygous mutant α6 subunit expression) or $0.5^{\alpha6}:0.5^{\alpha6(R46W)}:1^{\beta2}:1^{\gamma2L/\delta}$ (heterozygous wild-type and mutant α6 subunit expression) using the FuGENE 5 transfection reagent (Roche Applied Science, Indianapolis, IN, USA) according to the manufacturer's instructions. The terms 'heterozygous' and 'homozygous' are used solely to refer to

© 2011 The Authors. Journal compilation © 2011 The Physiological Society

mixed wild-type and mutant α6 subunit or pure mutant α6 subunit transfection, respectively. Cells were used 24–72 h after transfection. As a marker for successfully transfected cells, cDNA encoding green fluorescent protein was cotransfected together with the subunits of interest. For the surface expression measurement using flow cytometry, cells were first passaged onto 60 mm dishes and transfected 24 h later with 1 μg of each subunit in a ratio of 1:1:1 (homozygous α6 subunit expression) or 0.5:0.5:1:1 (heterozygous α6 subunit expression) with FuGENE 5 transfection reagent as previously described (Lo *et al.* 2008). Experiments were performed over the subsequent 2–3 days.

Whole-cell electrophysiology

Whole-cell voltage-clamp recordings were performed on lifted cells or outside-out membrane patches excised from transfected HEK 293T cells as described previously (Bianchi *et al.* 2001). Cells were bathed in an external solution consisting of (mM): NaCl 142, $CaCl_2$ 1, KCl 8, $MgCl_2$ 6, glucose 10, Hepes 10 (pH 7.4, ∼325 mosmol l^{-1}). Glass micropipettes were pulled from thin-walled borosilicate glass (World Precision Instruments, Sarasota, FL, USA) using a P2000 laser electrode puller (Sutter Instruments, San Rafael, CA, USA) and fire polished with a microforge (Narishige, East Meadow, NY, USA). Patch electrodes had resistances of 1–2 MΩ when filled with an internal solution consisting of (mM): KCl 153, $MgCl_2$ 1, Hepes 10, EGTA 5, Mg^{2+}-ATP 2 (pH 7.3, ∼300 mosmol l^{-1}). This combination of external and internal solutions produced a chloride equilibrium potential of ∼0 mV. Lifted cells were voltage-clamped at –20 mV and outside-out membrane patches at –50 mV using an Axopatch 200B amplifier (Axon Instruments, Union City, CA, USA). No voltage-dependent changes in kinetics were detected between –20 and –50 mV. GABA was applied to the lifted cells and/or excised macropatches using four-barrel square glass pipettes

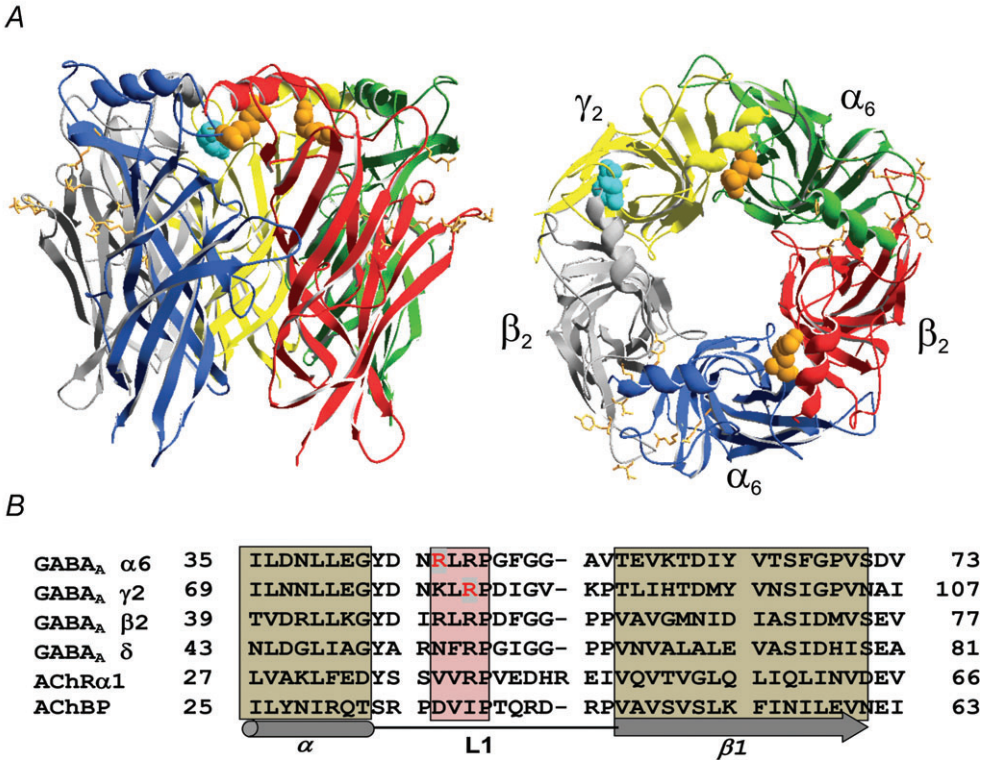

Figure 1. The α6 subunit mutation, R46W, contributes to the α/β and α/γ subunit interfaces in assembled $GABA_A$ receptors
A, a structural model of the N-terminal extracellular domain of human β2α6β2α6γ2 receptors viewed from outside the pentamer (left panel) and orthogonal toward the membrane (right panel) was developed. Mutations at α6R46 (in orange) and γ2R82 (in aqua) on the L1-loop at the α/β, α/γ and γ/β interfaces are shown in a space-fill representation. Residues involved in GABA binding at the β/α interface are shown as well (in orange in a stick representation). *B*, sequence alignments of the α-helix, L1-loop and the β1-sheet domain of human α6, β2, γ2 and δ subunits from the GABAR family, the nicotinic acetylcholine receptor α1 subunit (AChRα1) and the acetylcholine-binding protein (AChBP) are presented. The basic charged residues linked to CAE are shown in red within a pink box representing conserved residues into the L1-loop, and the light grey boxes represent residues in the α-helix and β1-sheet across the subunits.

© 2011 The Authors. Journal compilation © 2011 The Physiological Society

(Friedrich and Dimmock, Millville, NJ, USA) attached to a Warner SF-77B Perfusion Fast-Step (Warner Instrument Corporation, Hamden, CT, USA), which was commanded by Clampex 9.0 software (Axon Instruments). The solution exchange time across the open electrode tip was ∼400 μs. All experiments were performed at room temperature (22–23°C).

Currents were low-pass filtered at 2 kHz, digitized at 5–10 kHz, and analysed using the pCLAMP 9 software suite. Current amplitudes and 10–90% rise times were measured using Clampfit 9. Desensitization and deactivation current time courses were fitted using the Levenberg–Marquardt least squares method with up to four component exponential functions of the form $\sum a_n \exp(-t/\tau_n) + C$, where n is the number of the exponential components, t is time, a is the relative amplitude, τ_n is the time constant, and C is the residual current at the end of the GABA application. Additional components were accepted only if they significantly improved the fit, as determined by an F test on the sum of squared residuals. The time course of deactivation was summarized as a weighted time constant, defined by the following expression: $\sum a_n \tau_n / \sum a_n$. The extent of desensitization was measured as (fitted peak current – fitted steady-state current)/(fitted peak current). Numerical data were expressed as mean ± SEM. Statistical analysis was performed using Prism version 5.04 (GraphPad Software, La Jolla, CA, USA). Statistical significance was taken as $P < 0.05$, using unpaired two-tailed Student's t test or one-way ANOVA as appropriate.

Single-channel electrophysiology

Single-channel currents were recorded in cell-attached configuration as described previously (Tang *et al.* 2010). Cells were bathed in an external solution consisting of (mM): 140 NaCl, 5 KCl, 1 $MgCl_2$, 2 $CaCl_2$, 10 glucose, and 10 Hepes (pH 7.4). During recording, 1 mM GABA was present in the electrode solution consisting of (mM): 120 NaCl, 5 KCl, 10 $MgCl_2$, 0.1 $CaCl_2$, 10 glucose, and 10 Hepes (pH 7.4). The electrode potential was held at +80 mV. All experiments were conducted at room temperature.

Single-channel currents were amplified and low-pass filtered at 2 kHz using an Axopatch 200B amplifier, digitized at 20 kHz using Digidata 1322A, and saved using pCLAMP 9. Data were analysed using TAC 4.2 (Bruxton Corporation, Seattle, WA). Open and closed events were analysed using the 50% threshold detection method. All events were carefully checked visually before being accepted. Only patches showing no overlaps of simultaneous openings were accepted. Open and closed time histograms as well as amplitude histograms were generated using TACFit 4.2 (Bruxton Corporation, Seattle, WA, USA). Single-channel amplitudes (i) were calculated by fitting all-point histograms with single- or multi-Gaussian curves. The difference between the fitted 'closed' and 'open' peaks was taken as i. Duration histograms were fitted with exponential components in the form: $\sum (A_i/\tau_i)\exp(-t/\tau_i)$, where A and τ are the relative area and the time constant of the i component, respectively, and t is the time. The mean open time was then calculated as follows: $\sum A_i \tau_i$. The number of components required to fit the duration histograms was increased until an additional component did not significantly improve the fit (Fisher & Macdonald, 1997). Single-channel openings occurred as bursts of one or more openings or clusters of bursts. Bursts were defined as one or more consecutive openings that were separated by closed times that were shorter than a specified critical duration (t_{crit}) prior to and following the openings (Twyman *et al.* 1990). A t_{crit} duration of 5 ms was used in the current study. Clusters were defined as a series of bursts preceded and followed by closed intervals longer than a specific critical duration ($t_{cluster}$). A $t_{cluster}$ of 10 ms was used in this study. Data were expressed as the mean ± SEM. Statistical analysis was performed as described in the previous section.

Flow cytometry

Cells were harvested ∼48 h after transfection using 37°C trypsin-EDTA and placed immediately on ice in 4°C FACS buffer (Ca^{2+}/Mg^{2+}-free PBS with 2% FBS and 0.05% NaN_3). Cells were then pelleted by centrifugation, resuspended in 4°C FACS buffer, and transferred to 96-well polystyrene V-bottom plates. For measurements of subunit surface expression, cells were stained for 1 h on ice using primary antibodies diluted in 4°C FACS buffer and then washed 3 times in 4°C FACS buffer. Where necessary, cells were then stained for 1 h on ice using fluorophore-conjugated secondary antibodies before fixation in 2% w/v paraformaldehyde diluted in PBS. For measurements of total cellular expression, cells were harvested as described for surface staining. Prior to staining, however, cells were permeabilized for 15 min using Cytofix/Cytoperm fixation/permeabilization buffer and washed 2 times using Perm/Wash staining buffer (BD Biosciences, San Jose, CA, USA). Samples were then stained using primary antibodies diluted in 4°C Perm/Wash for 1 h on ice before being washed 4 times in 4°C Perm/Wash, 2 times in 4°C FACS buffer, and fixed in 2% w/v paraformaldehyde.

Expression levels were measured using a LSRII 3-laser flow cytometer (BD Biosciences, Sparks, MD, USA). Data were acquired using FACS-Diva (BD Biosciences) and analysed offline using FlowJo 7.5.5 (Tree Star Inc., Ashland, OR, USA). For each condition, 30,000 cells were analysed. Non-viable cells were excluded

© 2011 The Authors. Journal compilation © 2011 The Physiological Society

from analysis based on forward- and side-scatter properties, as determined in separate experiments by 7-amino-actinomycin-D staining. For each condition, the mean fluorescence obtained from staining cells transfected with empty pcDNA 3.1 was subtracted and the data were normalized to the wild-type $\alpha6\beta2\gamma2L/\delta$ condition for comparison. Statistical significance was determined using Student's unpaired *t* test.

Homology modelling

Three-dimensional models of human α6, β2, γ2 and δ subunit N-terminal domains were generated using the crystal structure of the N-terminal domain of the nAChR α subunit (Dellisanti *et al.* 2007) as a template (Protein Database accession number 2qc1) using the program SWISS-MODEL (Schwede *et al.* 2003). The initial sequence alignments between $GABA_A$ receptor subunits and the nAChR α subunit were generated with full-length multiple alignments using ClustalW (European Bioinformatics Institute, Hinxton, UK). Then the alignment of a 212-residue core of N-terminal domains of $GABA_A$ receptor subunits with residues of the N-terminal domain of the nAChR α subunit were submitted for automated comparative protein modelling implemented in the program suite incorporated in SWISS-MODEL (http://swissmodel.expasy.org/SWISS-MODEL.html) using the $GABA_A$ receptors sequence as a target protein and the nAChR sequence as a template structure. The α6 mutant structural model was individually made by selecting the mutation desired using the program DeepView/Swiss-PdbViewer 4.02 (Swiss Institute of Bioinformatics, Lausanne, Switzerland). SWISS-MODEL project files containing the target sequence with a single mutation, and the superposed template structure, were then modelled and submitted in the program. To generate pentameric $GABA_A$ receptor homology models, α6, β2 and γ2 or δ subunit N-terminal domain models were assembled in a counter-clockwise β2-α6-β2-α6-γ2/δ order by superposition onto the ACh binding protein as a template (Protein Database accession number 1i9b) (Brejc *et al.* 2001). The resulting models were subsequently energy-optimized using GROMOS96 in default settings within DeepView/Swiss-PdbViewer. The models with the most likely conformation were presented here.

Reagents

Reagents used included GABA (Sigma-Aldrich, St Louis, MO, USA), DMEM (Invitrogen), fetal bovine serum (Gibco, Billings, MT, USA), penicillin/streptomycin (Invitrogen), trypsin/EDTA (Gibco). Mouse monoclonal anti-β2/3 antibody (Clone 62-3G1) was obtained from Upstate (Lake Placid, NY, USA) and used at a dilution of 1:100 (surface) or 1:200 (total). Mouse monoclonal anti-HA antibody (clone 16B12) and Alexa647 labelling kits were obtained from Invitrogen and conjugated per manufacturer's instructions; the product was used at a dilution of 1:200 (surface) or 1:400 (total). Two different anti-FLAG antibodies (both clone M2) were used to verify results and optimize signal: conjugated anti-FLAG-Alexa647 antibody was obtained from Cell Signalling Technology (Beverly, MA, USA) and used at a dilution of 1:50 (surface) and 1:100 (total), and unconjugated anti-FLAG antibody was obtained from Sigma-Aldrich and used at dilution of 1:1000 (surface). Surface staining with unconjugated antibodies was followed by secondary antibody staining with Alexa647-conjugated goat anti-mouse IgG1 antibody (Invitrogen) as described previously. Total staining with unconjugated anti-β2/3 was performed using Alexa647-conjugated Zenon (Invitrogen) per manufacturer's instructions.

Results

The α6 subunit mutation, R46W, decreased current amplitude and altered the time course of transient $\alpha6\beta2\gamma2L$ receptor currents

We initially characterized the effect of the α6 subunit mutation, R46W, on macroscopic $\alpha6\beta2\gamma2L$ receptor currents. Whole-cell currents were elicited from lifted HEK 293T cells cotransfected with human β2 and γ2L subunits and wild-type α6 or mutant α6(R46W) subunits by applying a saturating GABA concentration (1 mM) for 400 ms using a rapid concentration jump technique (Fig. 2*A*). Peak $\alpha6(R46W)\beta2\gamma2L$ receptor current density (89 ± 14 pA pF^{-1}, $n = 18$, $P < 0.001$) was reduced relative to peak $\alpha6\beta2\gamma2L$ receptor current density (395 ± 53 pA pF^{-1}, $n = 21$) (Fig. 2*A* and *B*). To characterize the effects of the α6 subunit mutation, R46W, on macroscopic current kinetic properties (rate of activation (10–90% rise time), desensitization (current relaxation in the presence of saturating agonist) and deactivation (current relaxation after removal of agonist)) of $\alpha6(R46W)\beta2\gamma2L$ currents, we applied a saturating GABA concentration (1 mM) for 400 ms to excised outside-out patches obtained from cells expressing wild-type and mutant receptors (Fig. 2*C*). Again peak mutant receptor currents were smaller (400 ± 29.6 pA) than wild-type receptor currents (1427 ± 298 pA, $P < 0.001$). Mutant receptor current activation was slower than wild-type receptor current activation ($P < 0.01$, Table 1), and desensitization of mutant receptor currents was slightly more extensive ($35 \pm 2\%$) than that of wild-type receptor currents ($29 \pm 2\%$, $P < 0.05$, Fig. 2*D*, top left panel).

© 2011 The Authors. Journal compilation © 2011 The Physiological Society

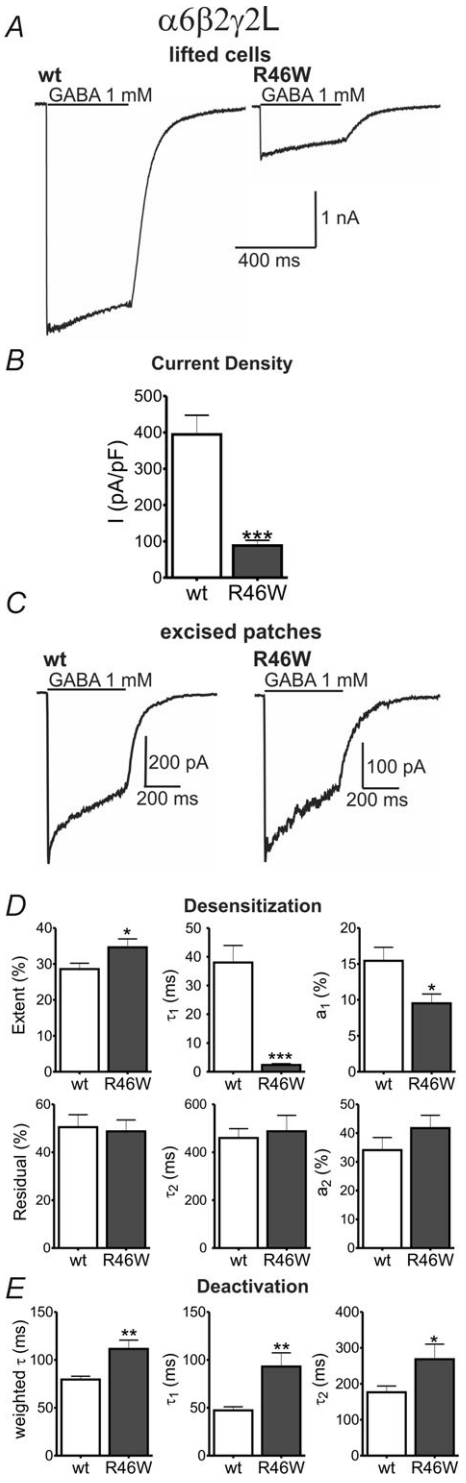

Figure 2. The R46W mutation evoked small $\alpha6\beta2\gamma2$L receptor currents with slowed activation and deactivation macroscopic kinetics
A, current responses to 400 ms pulses of 1 mM GABA to lifted cells containing wild-type (wt) and mutant R46W $\alpha6\beta2\gamma2$L receptors are shown. *B*, current densities of wild-type (white bars) and mutant R46W (grey bars) $\alpha6\beta2\gamma2$L receptors evoked by 400 ms pulses of 1 mM GABA to lifted cells are shown. *C*, current responses to 400 ms pulses of 1 mM GABA to excised patch cells containing wild-type and mutant R46W $\alpha6\beta2\gamma2$L receptors. *D* and *E*, summary of macroscopic kinetic parameters obtained from currents evoked by 400 ms pulses of 1 mM GABA to excised patches for both wild-type (white bars) and mutant R46W (grey bars) $\alpha6\beta2\gamma2$L receptors. Values represent mean ± SEM. Differences between wild-type and mutant channels are shown as *, ** and ***, which indicate $P < 0.05$, $P < 0.01$ and $P < 0.001$ (unpaired *t* test).

Table 1. Macroscopic kinetics of $\alpha6\beta2\gamma2$L currents after 400 ms applications of 1 mM GABA

	Excised outside-out macropatches (*n*)	
	wt (26)	R46W (22)
Rise time 10–90% (ms)	1.84 ± 0.12	2.56 ± 0.25**
Desensitization		
Extent (%)	29 ± 2	35 ± 2*
τ_1 (ms)	37.9 ± 5.93	2.36 ± 0.46***
τ_2 (ms)	460 ± 38.7	488 ± 66.5
a_1 (%)	15 ± 2	10 ± 1*
a_2 (%)	34 ± 4	42 ± 4
Residual (%)	50 ± 5	49 ± 5
Deactivation		
τ_1 (ms)	47.3 ± 3.77	93.0 ± 14.3**
τ_2 (ms)	176 ± 17.4	268 ± 42.2*
a_1 (%)	60 ± 5	68 ± 5
τ_{Weight} (ms)	79.4 ± 3.48	111 ± 9.22**

Values represent mean ± SEM. *, ** and *** indicate $P < 0.05$, $P < 0.01$ and $P < 0.001$ (unpaired *t* test) statistically different from wt, respectively.

Interestingly the increased extent of desensitization was not accompanied by a decrease in the relative contribution of the residual currents ($P > 0.05$, Fig. 2*D*, bottom left panel, Table 1). Both wild-type and mutant receptor currents desensitized with fast and slow exponential components (Fig. 2*D*, top central and right panels). The fast component time constant (τ_1; $P < 0.001$, Table 1) and relative contribution (a_1; $P < 0.001$, Table 1) for mutant receptor currents was much smaller than that for wild-type receptor currents (Fig. 2*D*, top right panels), but no differences in time constant (τ_2) or relative contribution (a_2) of the second exponential component were found ($P > 0.05$, Fig. 2*D*, bottom right panels, Table 1).

Deactivation of mutant receptor currents was significantly slower than for wild-type receptor currents (Fig. 2*E*, left panel). The slowing of mutant receptor current deactivation was due to larger deactivation time constants τ_1 and τ_2 ($P < 0.01$, $P < 0.05$, Table 1, Fig. 2*E*, middle and right panels) resulting in a larger weighted decay time constant ($P < 0.01$, Table 1, Fig. 2*E*, left panel). No differences were found in the relative contribution (a_1) of the first deactivation component

© 2011 The Authors. Journal compilation © 2011 The Physiological Society

for wild-type or mutant receptors ($P > 0.05$, Table 1). The longer deactivation time course displayed by mutant receptor currents may have been related to increased time for equilibration among desensitized states (Haas & Macdonald, 1999).

The α6 subunit mutation, R46W, decreased mean open time but increased opening frequency of single-channel α6β2γ2L currents

Modifications of macroscopic current kinetic properties may be due to alterations in single-channel gating properties. Thus cell-attached patches were obtained from HEK 293T cells expressing $\alpha6\beta2\gamma2$L or $\alpha6$(R46W)$\beta2\gamma2$L receptors. Steady-state on-cell single-channel recordings were obtained in the continuous presence of GABA (1 mM). Single-channel openings and complex bursting patterns were recorded from both wild-type (Fig. 3*A*, wt) and mutant (Fig. 3*A*, R46W) receptors. Wild-type receptor channels displayed brief bursts of openings and frequent prolonged (1–2 s) clusters of bursts; in contrast, mutant receptor channel openings occurred as single events and frequent brief bursts of openings. In addition, there was a small, but significant, difference between wild-type and mutant single-channel current amplitudes (Fig. 3*A* and *B*). Mutant receptor single-channel openings were briefer than wild-type receptor single-channel openings ($P < 0.01$, Table 2). This difference might represent a variation in the main conductance state of $\alpha6\beta2\gamma2$L receptors, which was 21–27 pS. Similar results were found in our previous reports for $\alpha\beta\gamma$ receptors expressed in mouse L929 cells (Angelotti & Macdonald, 1993; Fisher & Macdonald, 1997). Indeed, to rule out the possibility that these conductance levels were due to the presence of $\alpha\beta$ receptor currents, single-channel $\alpha6\beta2$ currents were recorded from HEK 293T cells in the presence of GABA (1 mM). $\alpha6\beta2$ receptors opened to a main current amplitude of 0.86 ± 0.11 pA ($n = 5$, $P < 0.001$ *vs.* wild-type, $P < 0.01$ *vs.* R46W), consistent with an ~12 pS channel conductance and in agreement with conductance levels for single-channel $\alpha1\beta2$ currents reported previously (Angelotti & Macdonald, 1993). The twofold difference in current amplitudes between $\alpha6\beta2$ and $\alpha6\beta2\gamma2$L single channels excludes the presence of a binary receptor population in our recordings.

To further address how the α6 subunit mutation, R46W, affected channel gating, we measured mean open time and opening frequency of both wild-type and mutant receptor single-channel currents. Overall, mutant receptor channels displayed lower mean open times (Fig. 3*C*) and higher opening frequencies (Fig. 3*D*) than wild-type receptor channels ($P < 0.05$, $P < 0.001$, Table 2). Open time distributions from wild-type and mutant receptors were fitted best by three exponential components (Fig. 3*E*). While there were no significant differences among the three open time constants (τ_1, τ_2 and τ_3) from wild-type and mutant receptors ($P > 0.05$, Table 2), there was a significant shift in the relative occurrence of the three components (a_{o1}, a_{o2} and a_{o3}) that accounted for the differences in mean open time of wild-type and mutant receptors. Mutant receptor single-channel openings were dominated by the shortest open state, accounting for ~78% of the relative area (a_{o1}) ($P < 0.001$, Table 2). In contrast, wild-type receptor single-channel openings contained a short open state that

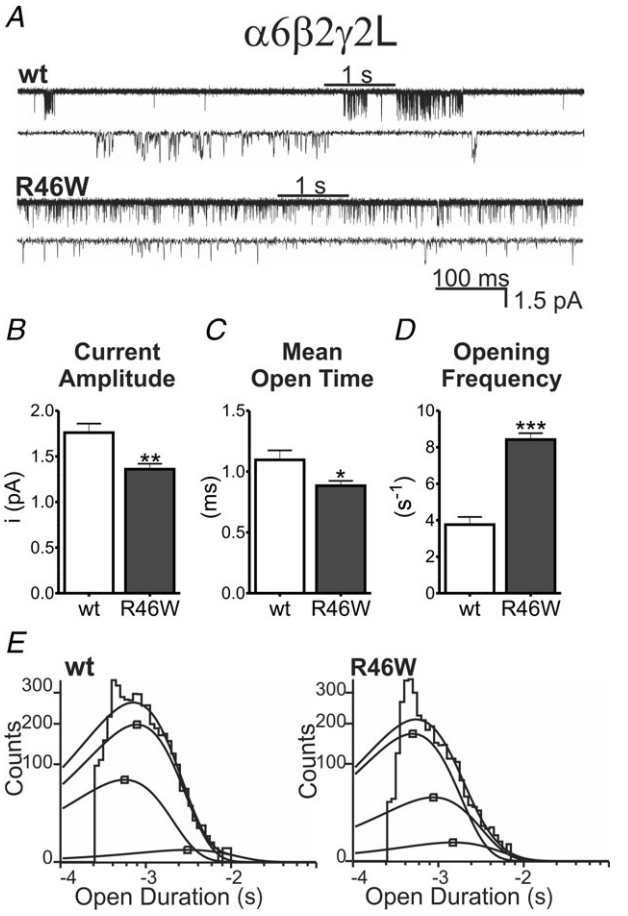

Figure 3. The R46W mutation affected gating efficacy by decreasing mean open time of single-channel α6β2γ2L currents
A, steady-state single-channel currents were obtained from cell-attached patches containing wild-type (wt) and mutant R46W $\alpha6\beta2\gamma2$L receptors. Patches were voltage clamped at +80 mV and continuously exposed to 1 mM GABA. Note that the upper traces in *A* (1 s, black bars) were expanded below them. *B–D*, single-channel kinetics for both wild-type (white bars) and mutant R46W (grey bars) $\alpha6\beta2\gamma2$L receptors are shown. *E*, representative open duration histograms for both wild-type and mutant R46W $\alpha6\beta2\gamma2$L receptors were fitted to three exponential functions. Values represent mean ± SEM. Differences between wild-type and mutant channels are shown as *, ** and ***, which indicate $P < 0.05$, $P < 0.01$ and $P < 0.001$ (unpaired *t* test).

© 2011 The Authors. Journal compilation © 2011 The Physiological Society

Table 2. Kinetic properties of $\alpha6\beta2\gamma2$L and $\alpha6\beta2\delta$ single-channel currents

	$\alpha6\beta2\gamma2$L (*n*)		$\alpha6\beta2\delta$ (*n*)	
	wt (8)	R46W (6)	wt (7)	R46W (6)
Channel amplitude (pA)	1.76 ± 0.09	1.36 ± 0.05**	1.69 ± 0.02	1.62 ± 0.05
Mean open time (ms)	1.09 ± 0.08	0.88 ± 0.04*	1.20 ± 0.11	0.89 ± 0.05*
Opening frequency (s^{-1})	3.76 ± 0.42	8.42 ± 0.35***	10.1 ± 1.81	2.77 ± 0.54**
Open time constants				
τ_{o1} (ms)	0.62 ± 0.04	0.56 ± 0.05	0.60 ± 0.02	0.44 ± 0.02***
τ_{o2} (ms)	0.75 ± 0.09	0.61 ± 0.06	0.86 ± 0.08	0.58 ± 0.02*
τ_{o3} (ms)	2.28 ± 0.31	1.81 ± 0.12	2.18 ± 0.17	2.17 ± 0.12
a_{o1} (%)	25 ± 3	78 ± 6***	14 ± 1	25 ± 2***
a_{o2} (%)	71 ± 4	19 ± 5***	81 ± 2	71 ± 2**
a_{o3} (%)	4 ± 2	3 ± 1	5 ± 1	4 ± 1
Intraburst closed time constant				
τ_{c1} (ms)	1.37 ± 0.17	1.21 ± 0.13	0.75 ± 0.05	0.59 ± 0.04*
τ_{c2} (ms)	5.40 ± 0.72	6.53 ± 1.03	4.79 ± 0.49	2.53 ± 0.50*
a_{c1} (%)	50 ± 4	28 ± 4**	11 ± 1	7 ± 2
a_{c2} (%)	36 ± 4	45 ± 3	22 ± 3	15 ± 3
Burst kinetics				
Openings per burst	3.03 ± 0.24	2.27 ± 0.26	1.75 ± 0.21	1.33 ± 0.12
P_o	0.010 ± 0.003	0.013 ± 0.002	0.018 ± 0.002	0.003 ± 0.001**
Duration (ms)	6.66 ± 0.57	3.80 ± 0.12**	2.90 ± 0.11	1.43 ± 0.12***
Frequency (s^{-1})	1.28 ± 0.13	3.93 ± 0.39***	6.02 ± 1.29	2.18 ± 0.48*
τ_1 (ms)	0.82 ± 0.03	0.74 ± 0.04	0.61 ± 0.04	0.54 ± 0.04
τ_2 (ms)	10.1 ± 1.00	6.68 ± 0.43*	5.87 ± 0.76	3.23 ± 0.21*
a_1 (%)	35 ± 2	50 ± 2***	64 ± 2	82 ± 2***
a_2 (%)	65 ± 2	51 ± 2***	36 ± 2	18 ± 2***

Values represent mean ± SEM. *, ** and *** indicate $P < 0.05$, $P < 0.01$ and $P < 0.001$ (unpaired *t* test) statistically different from wt, respectively.

accounted for only ∼25% of the single-channel openings, and a longer open state that accounted for ∼71% of the relative area (a_{o2}) ($P < 0.001$, Table 2). No differences were found in the relative area of the longest open state (a_{o3}) ($P > 0.05$, Table 2).

The α6 subunit mutation, R46W, decreased burst duration and increased burst frequency of $\alpha6\beta2\gamma2$L single-channel currents

In response to saturating concentrations of GABA, $GABA_A$ receptor channels display bursts of fast transitions between open and closed states prior to unbinding of agonist or entering into desensitized states. To determine the effects of the α6 subunit mutation, R46W, on single-channel bursts, we analysed the intraburst kinetics of single-channel currents from $\alpha6\beta2\gamma2$L and $\alpha6$(R46W)$\beta2\gamma2$L receptor channels. First we focused on the two briefest closed time constants that most likely represent closures within bursts of channel activity (Twyman *et al.* 1990). Interestingly, both intraburst closed time constants (τ_{c1} and τ_{c2}) for mutant receptors were similar to those found for wild-type receptors ($P > 0.05$, Table 2), but the relative contribution of the brief component (a_{c1}) for mutant receptors was significantly reduced relative to wild-type receptors ($P < 0.01$, Table 2). Thus, agonist activation of mutant receptors produced single-channel currents with bursts that usually occurred as single openings or brief bursts of openings and closings, while wild-type receptors produced single-channel openings that contained prolonged bursts of brief openings. The duration of bursts was reduced for mutant receptors relative to wild-type receptors (see representative 200 ms traces of bursting wild-type (Fig. 4*A*, wt) and mutant (Fig. 4*A*, R46W) receptor currents). Further analysis showed that burst durations of mutant receptor currents were significantly reduced relative to wild-type receptor currents ($P < 0.01$, Table 2, Fig. 4*B*), and this difference was associated with a slight reduction of openings per burst ($P > 0.05$, Table 2) and a substantial increase in burst frequency of mutant receptor currents ($P < 0.001$, Table 2, Fig. 4*C*).

The burst duration frequency distributions were fitted best by two exponential functions for both wild-type and mutant receptors (Fig. 4*D*). However, there were no differences in the time constants for the short-duration burst component (τ_1) for the receptors ($P > 0.05$, Table 2,

© 2011 The Authors. Journal compilation © 2011 The Physiological Society

Fig. 4*E*, left panel), but the time constant for the longer-duration burst component (τ_2) was significantly reduced for mutant receptors ($P < 0.05$, Table 2, Fig. 4*E*, right panel). In addition, with mutant receptors there was a shift in the distribution of the two populations of burst durations due to an increase in the relative proportion of bursts with short duration (a_1) and a reduction in the relative proportion of longer bursts (a_2) ($P < 0.001$, Table 2, Fig. 4*F*). Taken together, mutant receptor burst durations were reduced due to reduction of the time that the channel spends in the open state.

The α6 subunit mutation, R46W, decreased surface expression of α6β2γ2L receptors

To gain insight into the effects of the α6 subunit mutation, R46W, on GABA$_A$ receptor assembly, wild-type $\alpha6^{FLAG}$ and mutant $\alpha6(R46W)^{FLAG}$ subunits were coexpressed in HEK 293T cells, and surface and total expression levels of each subunit were assessed using flow cytometry (Fig. 5*A* and *C*). Coexpression of $\alpha6(R46W)^{FLAG}$ with β2 and $\gamma2L^{HA}$ subunits resulted in a significant reduction of both $\alpha6(R46W)^{FLAG}$ and β2, but not $\gamma2L^{HA}$, subunits on the cell surface (Fig. 5*A*). Cell surface levels of mutant $\alpha6(R46W)^{FLAG}$ subunits were reduced compared to wild-type $\alpha6^{FLAG}$ subunits (0.69 ± 0.04, $n = 10$ compared to 1.00 ± 0.002, $n = 10$, respectively, $P < 0.001$, Fig. 5*B*, left panel), and β2 subunits were also reduced compared to control subunits when coexpressed with mutant $\alpha6(R46W)^{FLAG}$ subunits (0.81 ± 0.02, $n = 10$ compared to 0.995 ± 0.002, $n = 10$, respectively, $P < 0.001$, Fig. 5*B*, middle panel). No differences were found in surface levels of $\gamma2L^{HA}$ subunits (1.10 ± 0.05, $n = 10$ compared to 0.998 ± 0.001, $n = 10$, respectively, $P > 0.05$, Fig. 5*B*, right panel).

Total cellular levels of coexpressed $\alpha6^{FLAG}$ or $\alpha6(R46W)^{FLAG}$ and β2, and $\gamma2L^{HA}$ subunits were measured by permeabilizing cell membranes prior to staining (Fig. 5*C*). Comparable to surface levels, when coexpressed with β2 and $\gamma2L^{HA}$ subunits total expression of $\alpha6(R46W)^{FLAG}$ subunits was reduced significantly relative to $\alpha6^{FLAG}$ subunits (0.37 ± 0.03, $n = 10$ compared to 1.0 ± 0.001, $n = 10$, respectively, $P < 0.001$, Fig. 5*D*, left panel). Interestingly, this reduction was associated with a reduction of total levels of $\gamma2L^{HA}$ subunits (0.67 ± 0.03, $n = 10$, $P < 0.001$, Fig. 5*D*, right panel), but with no changes in total levels of coexpressed β2 subunits (0.80 ± 0.10, $n = 7$, $P > 0.05$, Fig. 5*D*, middle panel).

These results suggested that the R46W mutation impaired expression and surface trafficking of α6 subunits. Moreover, α6(R46W) subunits had a dominant negative effect on partnering subunits, reducing surface expression of β2 subunits and total cellular expression of γ2L subunits. Importantly, though total α6(R46W) subunit levels were reduced, some α6(R46W) subunits could be successfully assembled with β2 and γ2L subunits into α6(R46W)β2γ2L receptors that were trafficked to the cell surface. However, because expression levels of α6(R46W), β2 and γ2L subunits were not affected equally, it is likely that the mutation led to the production of surface receptors with altered stoichiometry.

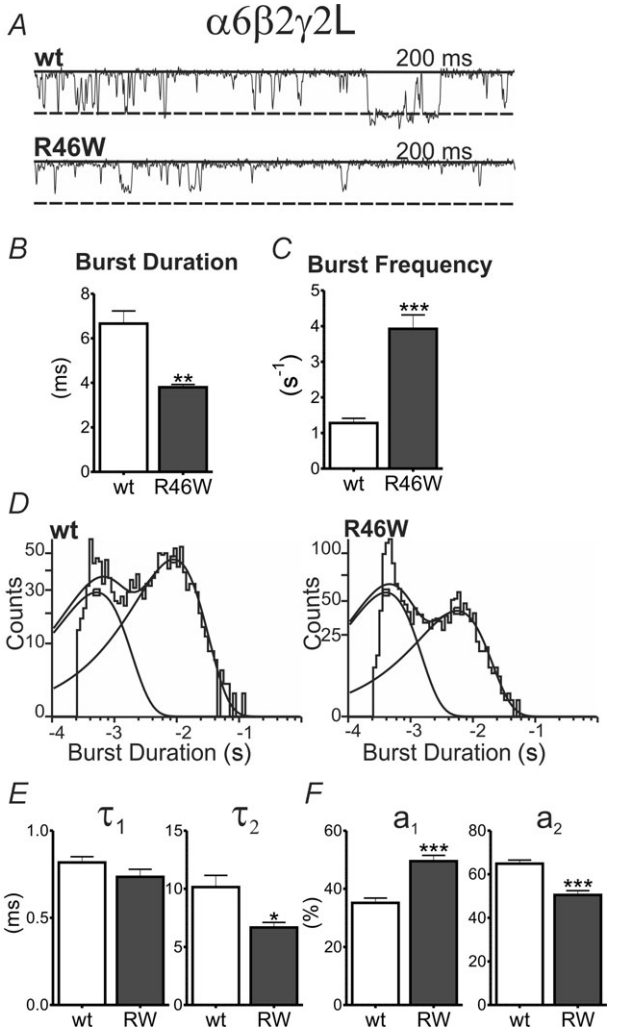

Figure 4. Mutant α6(R46W)β2γ2L receptor channel bursts occurred as brief single openings, which decreased single-channel current burst durations
A, representative steady-state single-channel current traces from cell-attached patches containing wild-type (wt) and mutant R46W α6β2γ2L receptors. Patches were voltage clamped at +80 mV and continuously exposed to 1 mM GABA. *B* and *C*, comparison of burst kinetics for both wild-type (white bars) and mutant R46W (grey bars) α6β2γ2L receptors are shown. *D*, representative burst duration histograms for both wild-type and mutant R46W receptors were fitted to two exponential functions. *E–F*, time constants (τ) and representative areas (*a*) of burst duration histograms for both wild-type (white bars) and mutant R46W receptors (grey bars) are shown. Values represent mean ± SEM. Differences between wild-type and mutant channels are shown as *, ** and ***, which indicate $P < 0.05$, $P < 0.01$ and $P < 0.001$ (unpaired *t* test).

© 2011 The Authors. Journal compilation © 2011 The Physiological Society

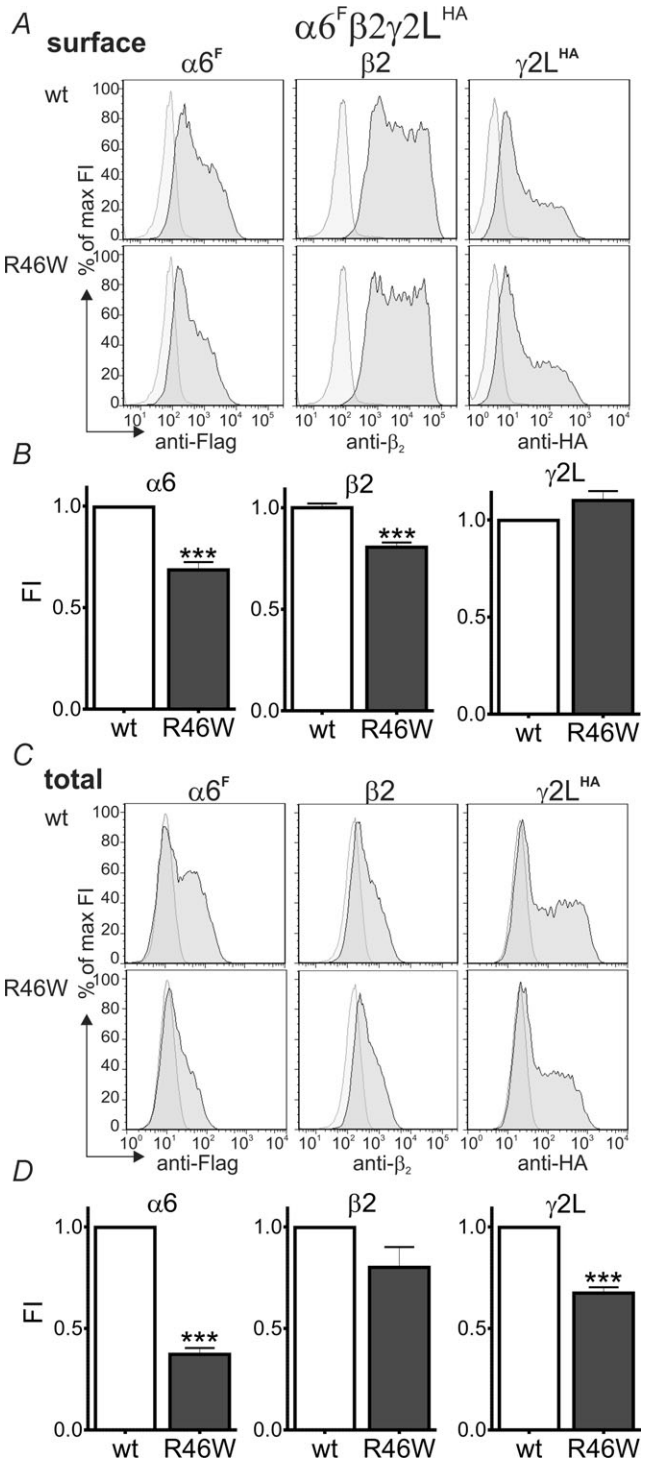

Figure 5. The R46W mutation decreased surface expression of α6 and β2, but not γ2L subunits of α6β2γ2L receptors
A, $GABA_A$ receptor $\alpha6^F$, $\alpha6^F$(R46W), $\beta2$ and $\gamma2L^{HA}$ subunit cell surface levels were measured by flow cytometry for cells coexpressing wild-type (wt) and mutant R46W $\alpha6\beta2\gamma2$L receptors. Representative histograms of positively transfected cells (dark grey) were superimposed on those from mock transfected cells (light grey) and shown for surface expression. Note that the abscissa has a log scale. *B*, the mean fluorescence intensity (FI) of $\alpha6$, $\beta2$ and $\gamma2$L subunit surface expression was quantified for wild-type (white bars) and mutant R46W receptors (grey bars). *C*, $GABA_A$ receptor $\alpha6^F$, $\alpha6^F$(R46W), $\beta2$ and $\gamma2L^{HA}$ subunit total cellular levels were measured by flow cytometry for cells coexpressing wild-type and mutant R46W $\alpha6\beta2\gamma2$L receptors. Representative histograms of positively transfected cells (dark grey) were superimposed on those from mock transfected cells (light grey). *D*, the mean fluorescence intensity (FI) of $\alpha6^F$, $\beta2$ and $\gamma2L^{HA}$ subunit total cell expression was quantified as well (wild-type as white bars, and mutant receptors as grey bars). Values represent mean ± SEM. Differences between wild-type and mutant channels are shown as ***, which indicate $P < 0.001$ (unpaired *t* test). ^{F}, FLAG.

Heterozygous coexpression of mutant α6(R46W) and wild-type α6 subunits with β2 and γ2L subunits produced intermediate macroscopic receptor current amplitudes

To determine the effect of heterozygous expression of wild-type $\alpha6$ and mutant $\alpha6$(R46W) subunits (50/50 mix of wild-type and mutant $\alpha6$ subunits) on $\alpha6\beta2\gamma2$L currents, we compared wild-type $\alpha6\beta2\gamma2$L, heterozygous $\alpha6/\alpha6$(R46W)$\beta2\gamma2$L and homozygous mutant $\alpha6$(R46W)$\beta2\gamma2$L receptor whole-cell currents elicited from lifted HEK 293T cells evoked by application of 4 second concentration jumps of saturating GABA (1 mM) (Fig. 6*A*). Heterozygous receptor currents were larger (Fig. 6*A* inset panel, $P < 0.001$, Table 3) and desensitized more extensively (Fig. 6*B* middle panel, $P < 0.01$, Table 3) than homozygous mutant receptor currents. In addition, the 10–90% activation rise time was shorter than for homozygous receptor currents (Fig. 6*B* left panel, $P < 0.001$, Table 3). When compared with wild-type receptors, heterozygous receptors had decreased maximal peak current density with no differences in the extent of desensitization or activation (Fig. 6*A* inset panel and *B*, Table 3).

The desensitization time courses of wild-type, heterozygous and homozygous mutant receptor currents were fitted best by four exponential components (Table 3). Despite the fact that both heterozygous and homozygous mutant receptor currents exhibited a significantly slower third component exponential time constant (τ_3) than wild-type receptor currents ($P < 0.05$, Table 3), heterozygous receptors displayed similar desensitization component distribution values (a_1, a_2, a_3 and a_4) and residuals compared to wild-type receptor currents ($P > 0.05$, Table 3), but significantly different from homozygous mutant receptor currents ($P < 0.01$, Table 3, Fig. 6*B* right panel). Moreover, heterozygous receptor currents deactivated faster than homozygous mutant receptor currents ($P < 0.01$, Table 3), but with kinetic properties similar to those of wild-type receptors.

© 2011 The Authors. Journal compilation © 2011 The Physiological Society

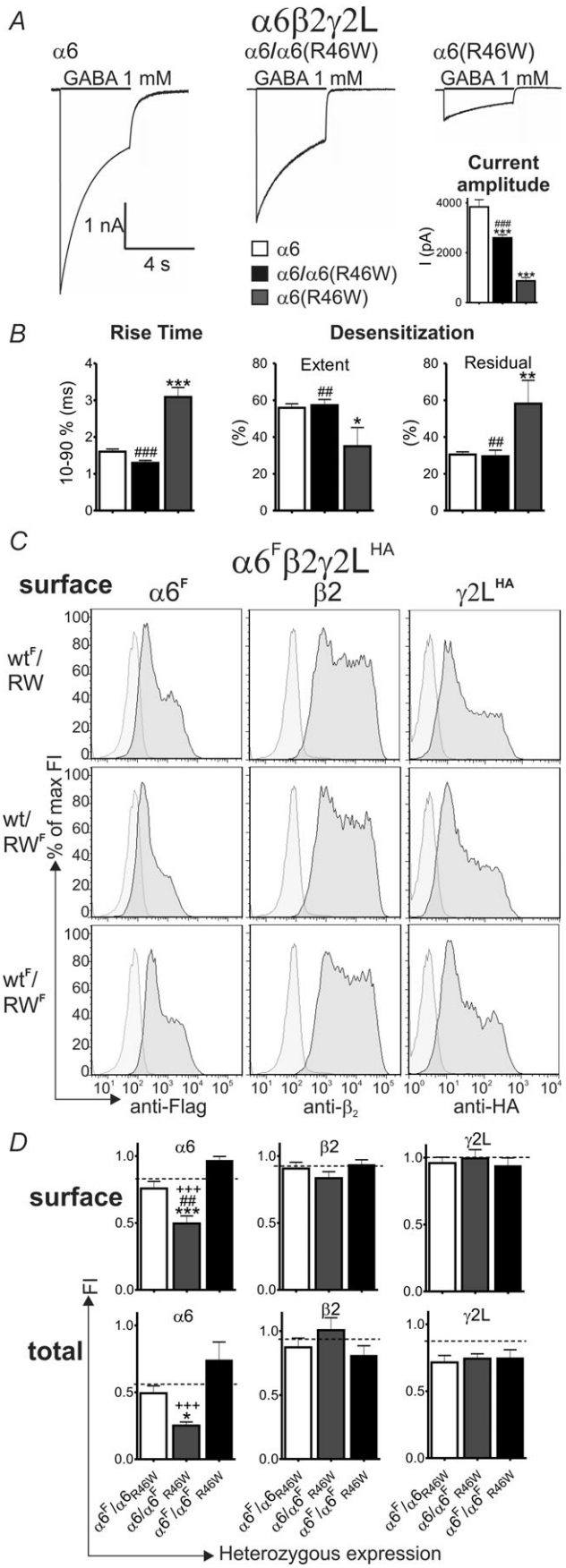

With heterozygous coexpression of mutant α6(R46W) and wild-type α6 subunits with β2 and γ2L subunits, there was increased incorporation of wild-type subunits over mutant subunits

To gain insight into the assembly fate of wild-type α6 and mutant α6(R46W) subunits with heterozygous expression, we coexpressed α6, α6(R46W), β2 and $\gamma2L^{HA}$ subunit cDNA at a molar ratio of 0.5:0.5:1:1 (see Methods) and evaluated subunit expression levels using flow cytometry (Fig. 6*C*). To distinguish wild-type and mutant subunits, we differentially tagged α6 and α6(R46W) subunits with the FLAG epitope. Specifically, we determined surface levels of wild-type and mutant α6 subunits coexpressed with β2 and γ2L subunits when only the wild-type subunit ($\alpha6^{FLAG}$/α6(R46W), Fig. 6*D* top left panel, white bar), only the mutant subunit (α6/α6(R46W)^{FLAG}, Fig. 6*D* top left panel, grey bar) or both subunits ($\alpha6^{FLAG}$/α6(R46W)^{FLAG}, Fig. 6*D* top left panel, black bar) were FLAG-tagged.

With the 'half-tagged' subunits, we compared FLAG-tagged subunit levels obtained with heterozygous expression to those obtained with coexpression of 'half-tagged' wild-type $\alpha6^{FLAG}$/α6 subunits (Fig. 6*D*, dotted line). Heterozygous expression of half-tagged $\alpha6^{FLAG}$/α6(R46W) subunits (Fig. 6*D*, top panel, white bars) resulted in no significant difference in surface levels of $\alpha6^{FLAG}$ (0.76 ± 0.05, $n = 7$, $P > 0.05$, Fig. 6*D*, left top panel), β2 (0.91 ± 0.05, $n = 8$, $P > 0.05$, Fig. 6*D*, middle top panel) or $\gamma2L^{HA}$ (0.96 ± 0.04, $n = 8$, $P > 0.05$, Fig. 6*D*,

Figure 6. Heterozygous coexpression of mutant α6(R46W) and wild-type α6 subunits produced intermediate macroscopic receptor current amplitudes by assembling a mixed fraction of wild-type/mutant receptors on the surface
A, current responses to long (4 s) applications of 1 mM GABA to lifted cells containing wild-type α6β2γ2L, heterozygous α6/α6(R46W)β2γ2L and α6(R46W)β2γ2L receptors are shown. In the inset, current amplitudes for α6 (white bar), α6/α6(R46W) (black bar) and α6(R46W) (grey bar) subunit-containing receptors are shown. *B*, the 10–90% rise time, extent of desensitization and residual current for currents evoked by 4 s pulses of 1 mM GABA are presented for wild-type, heterozygous and mutant α6β2γ2L receptors. *C*, surface levels of heterozygous $\alpha6^F$/α6(R46W) (wt^F/RW), α6/α6(R46W)^F (wt/RW^F) and $\alpha6^F$/α6(R46W)^F (wt^F/RW^F) subunits coexpressed with β2 and $\gamma2L^{HA}$ subunits were measured using flow cytometry. Histograms of positively transfected cells (dark grey) were superimposed on those from mock transfected cells (light grey). *D*, the mean fluorescence intensity (FI) of $\alpha6^F$, β2 and $\gamma2L^{HA}$ subunit surface and total levels were quantified for heterozygous $\alpha6^F$/α6(R46W), α6/α6(R46W)^F, and $\alpha6^F$/α6(R46W)^F subunit combinations. Dashed lines represent half-tagged $\alpha6^F$/α6 levels. Values represent mean ± SEM. *, ** and *** indicate $P < 0.05$, $P < 0.01$ and $P < 0.001$ (one-way ANOVA) statistically different from wild-type levels (α6 or $\alpha6^F$/α6), respectively. ## and ### indicate $P < 0.01$ and $P < 0.001$ (one-way ANOVA) statistically different from α6(R46W) or $\alpha6^F$/α6R46W. +++ indicates $P < 0.001$ (one-way ANOVA) statistically different from α6/α6R46W^F. ^{F}, FLAG.

© 2011 The Authors. Journal compilation © 2011 The Physiological Society

Table 3. Macroscopic kinetic properties of $\alpha6\beta2\gamma2$L and $\alpha6\beta2\delta$ currents evoked by 4 s applications of 1 mM GABA

	$\alpha6\beta2\gamma2$L (*n*)			$\alpha6\beta2\delta$ (*n*)	
	wt (15)	R46W (7)	wt/R46W (18)	wt (11)	R46W (6)
Rise time 10–90% (ms)	1.60 ± 0.07	3.09 ± 0.26***	1.30 ± 0.07###	2.82 ± 0.28	7.04 ± 1.23***
Current density (pA pF^{-1})	427 ± 31.6	96.8 ± 14.7***	289 ± 12.8***###	130 ± 5.66	2.84 ± 0.29***
Desensitization					
Extent (%)	56 ± 2	35 ± 10*	57 ± 3##	34 ± 4	2 ± 1***
τ_1 (ms)	2.32 ± 0.56	1.89 ± 0.39	1.92 ± 0.61	7.20 ± 2.53	NA
τ_2 (ms)	190 ± 35.1	171 ± 34.1	278 ± 41.1	85.2 ± 39.2	NA
τ_3 (ms)	528 ± 71.5	1312 ± 448.7*	1138 ± 155.2*	1606 ± 246.4	NA
τ_4 (ms)	2533 ± 386.1	2322 ± 287.2	2742 ± 257.0	2739 ± 378.4	NA
a_1 (%)	2 ± 0.3	12 ± 3***	2 ± 0.4###	6 ± 2	NA
a_2 (%)	3 ± 0.4	17 ± 6**	9 ± 2#	8 ± 2	NA
a_3 (%)	31 ± 7	5 ± 3*	33 ± 6#	7 ± 3	NA
a_4 (%)	45 ± 5	43 ± 11	50 ± 4	33 ± 6	NA
Residual (%)	31 ± 1	58 ± 13**	30 ± 3##	52 ± 7	NA
Deactivation					
τ_1 (ms)	75.1 ± 6.04	120 ± 28.1*	55.1 ± 3.45###	333 ± 10.6	14.0 ± 3.15***
τ_2 (ms)	430 ± 38.2	1050 ± 280.2**	400 ± 54.9###	1280 ± 153.0	403.3 ± 236.7**
a_1 (%)	88 ± 3	89 ± 3	90 ± 2	81 ± 3	71 ± 10
τ_{Weight} (ms)	96.2 ± 9.62	184 ± 65.1*	66.8 ± 3.14##	425 ± 10.4	25.0 ± 9.97***

Values represent mean ± SEM. *, ** and *** indicate $P < 0.05$, $P < 0.01$ and $P < 0.001$ (unpaired *t* test or one-way ANOVA) statistically different from wt, respectively. #, ## and ### indicate $P < 0.05$, $P < 0.01$ and $P < 0.001$ (one-way ANOVA) statistically different from α6R46Wβ2L. NA = not available.

right top panel) subunits, when compared to coexpression of half-tagged $\alpha6^{FLAG}/\alpha6$ subunits ($\alpha6^{FLAG} = 0.83 \pm 0.05$, $n = 7$, $\beta2 = 0.92 \pm 0.02$, $n = 7$, and $\gamma2L^{HA} = 1.00 \pm 0.03$, $n = 7$, respectively, Fig. 6*D*, top panels, dotted lines). These results suggested that incorporation of wild-type $\alpha6^{FLAG}$, $\beta2$ and $\gamma2L^{HA}$ subunits into heterozygous receptors was not affected by the presence of the mutant subunit or the FLAG tag.

Heterozygous expression of half-tagged $\alpha6/\alpha6(R46W)^{FLAG}$ subunits, however, resulted in a significant reduction of surface $\alpha6(R46W)^{FLAG}$ subunits (0.50 ± 0.06, $n = 7$, Fig. 6*D*, left top panel grey bar) relative to those obtained with wild-type $\alpha6^{FLAG}/\alpha6$ subunits ($P < 0.001$, Fig. 6*D*, left top panel, black bar) and with heterozygous $\alpha6^{FLAG}/\alpha6(R46W)$ subunits ($P < 0.01$, Fig. 6*D*, left top panel, white bar) levels. These results suggest that with heterozygous expression, both wild-type and mutant $\alpha6$ subunits could be incorporated into surface-trafficked receptors, but that wild-type subunits were preferred over mutant subunits.

With 'full-tagged' heterozygous $\alpha6^{FLAG}/\alpha6(R46W)^{FLAG}$ subunit coexpression, there was a small, non-significant increase in $\alpha6$ subunit levels on the cell surface (0.97 ± 0.03, $n = 6$, Fig. 6*D*, left top panel, black bar) relative to those obtained with half-tagged $\alpha6^{FLAG}/\alpha6(R46W)$ subunit coexpression (Fig. 6*D*, left top panel, white bar), again suggesting that with heterozygous expression, wild-type subunits are incorporated into the receptors much more successfully than mutant subunits.

As would be expected if the FLAG epitope did not disrupt overall assembly of the receptors, no significant differences were found in the surface expression levels of $\beta2$ (Fig. 6*D*, middle panel) (0.84 ± 0.04, $n = 8$, grey bar, and 0.93 ± 0.04, $n = 6$, black bar) or $\gamma2L$ (Fig. 6*D*, right panel) (0.99 ± 0.07, $n = 8$, grey bar, and 0.94 ± 0.06, $n = 6$, black bar) subunits with heterozygous coexpression of either $\alpha6/\alpha6(R46W)^{FLAG}$ or $\alpha6^{FLAG}/\alpha6(R46W)^{FLAG}$ subunits, respectively. Moreover, in all heterozygous conditions, neither $\beta2$ nor $\gamma2L$ subunit surface expression was reduced compared to levels obtained with coexpression of 'half-tagged' wild-type $\alpha6^{FLAG}/\alpha6$ subunits (Fig. 6*D*, top middle and right panels, all bars compared to dotted line). These data indicate that heterozygous expression of $\alpha6(R46W)$ subunits did not reduce surface expression levels of $\beta2$ or $\gamma2L$ subunits.

Using a similar approach, total cellular expression of heterozygous $\alpha6^{FLAG}/\alpha6(R46W)$, $\alpha6/\alpha6(R46W)^{FLAG}$, and $\alpha6^{FLAG}/\alpha6(R46W)^{FLAG}$ subunits coexpressed with $\beta2$ and $\gamma2L^{HA}$ subunits was measured (Fig. 6*D*, bottom panels). Similar to the cell surface results obtained for heterozygous coexpression of $\alpha6^{FLAG}/\alpha6(R46W)$ with $\beta2$ and $\gamma2L^{HA}$ subunits, no differences were found in total expression of $\alpha6^{FLAG}$ (0.49 ± 0.06, $n = 8$, $P > 0.05$, Fig. 6*D*, left bottom panel, white bar), $\beta2$ (0.87 ± 0.07, $n = 5$, $P > 0.05$, Fig. 6*D*, middle bottom panel, white bars) and $\gamma2L^{HA}$ (0.72 ± 0.05, $n = 8$, $P > 0.05$, Fig. 6*D*, right bottom panel, white bar) subunits, when compared to those obtained with coexpression of half-tagged $\alpha6^{FLAG}/\alpha6$ subunits

© 2011 The Authors. Journal compilation © 2011 The Physiological Society

($\alpha6^{FLAG} = 0.56 \pm 0.08$, $n = 7$, $\beta2 = 0.94 \pm 0.15$, $n = 4$, and $\gamma2L^{HA} = 0.88 \pm 0.08$, $n = 7$, respectively, dotted lines).

Coexpression of $\alpha6/\alpha6(R46W)^{FLAG}$ subunits, however, resulted in a larger reduction of total FLAG expression (0.25 ± 0.03, $n = 8$, Fig. 6*D*, left bottom panel, grey bar) than with either half-tagged wild-type ($\alpha6^{FLAG}/\alpha6 = 0.56 \pm 0.08$, $n = 7$, $P < 0.05$, Fig. 6*D*, left bottom panel, dotted line) or heterozygous $\alpha6^{FLAG}/\alpha6(R46W)$ ($P > 0.05$, Fig. 6*D*, left bottom panel, white bar) subunits. Again, when $\alpha6^{FLAG}/\alpha6(R46W)^{FLAG}$ subunits were coexpressed, there was an increase in total expression levels of FLAG expression (0.74 ± 0.14, $n = 6$, Fig. 6*D*, left bottom panel, black bar) relative to those obtained with expression of $\alpha6(R46W)^{FLAG}$ subunits ($P < 0.001$, Fig. 6*D*, left bottom panel, grey bar), indicating that both wild-type and mutant subunits were expressed. Similar to expression of $\alpha6^{FLAG}/\alpha6(R46W)^{FLAG}\beta2\gamma2L^{HA}$ receptors on the cell surface, there was also more total cell wild-type α6 subunits (~66%) than mutant α6(R46W) subunits (~34%).

As with surface expression, no significant differences were found for total expression levels of β2 (Fig. 6*D*, middle bottom panel) (1.00 ± 0.09, $n = 5$, grey bar, and 0.81 ± 0.08, $n = 3$, black bar) or γ2L (Fig. 6*D*, right bottom panel) (0.74 ± 0.04, $n = 8$, grey bar, and 0.75 ± 0.06, $n = 6$, black bar) subunits with heterozygous coexpression of either $\alpha6/\alpha6(R46W)^{FLAG}$ or $\alpha6^{FLAG}/\alpha6(R46W)^{FLAG}$ subunits, respectively. Taken together, these data suggest that when α6 and α6(R46W) subunits are 'heterozygously' coexpressed with β2 and γ2L subunits, all subunits are expressed, and the number of $GABA_A$ receptors on the cell surface is not affected. Those receptors may contain α6 and/or α6(R46W) subunits, but expression and incorporation of wild-type α6 subunits is preferred.

The α6 subunit mutation, R46W, decreased macroscopic α6β2δ receptor current amplitude by reducing single-channel mean open time and opening frequency

The α6 subunit has been shown to coassemble with both γ2 and δ subunits. To determine the effect of the α6 subunit mutation, R46W, on the macroscopic kinetic properties of α6β2δ currents, we compared wild-type α6β2δ and mutant α6(R46W)β2δ whole-cell currents elicited from lifted HEK 293T cells by applying 4 second concentration jumps of saturating GABA (1 mM) (Fig. 7*A*). Wild-type α6β2δ currents were smaller and desensitized less (Fig. 7*D*, Table 3) than α6β2γ2L receptor currents, consistent with the macroscopic properties of α6β3δ and α6β3γ2L receptor currents reported previously (Saxena & Macdonald, 1996). Mutant α6(R46W)β2δ receptor currents also had much smaller peak currents and less whole-cell current desensitization than mutant α6(R46W)β2γ2L receptor currents (Table 3). Mutant α6(R46W)β2δ receptor currents were reduced substantially relative to wild-type α6β3δ receptor currents ($P < 0.001$, Table 3, Fig. 7*A* and *B*), and their activation was slower than wild-type receptor currents ($P < 0.001$, Table 3, Fig. 7*C*). While wild-type α6β2δ receptor currents exhibited some slow desensitization that was best fitted by four exponential functions (Table 3), mutant α6(R46W)β2δ currents displayed negligible macroscopic desensitization ($P < 0.001$, Table 3, Fig. 7*D*). In addition, mutant α6(R46W)β2δ receptor currents had significantly faster current deactivation than wild-type α6β2δ receptor currents ($P < 0.001$, Table 3, Fig. 7*E*).

The severe alteration of macroscopic properties of α6(R46W)β2δ receptor currents should be due to altered single-channel currents. Thus, mutant α6(R46W)β2δ and wild-type α6β2δ single-channel currents evoked by steady-state application of 1 mM GABA were compared. Wild-type single channels opened in prolonged bursts (Fig. 7*F*, top panel), while mutant single channels opened less frequently in brief bursts (Fig. 7*F*, bottom panel). The single-channel open duration histograms for wild-type and mutant receptors were fitted best by the sum of three exponential functions (Fig. 7*G*). For both wild-type and mutant single-channel current open duration histograms, the time constant (τ_{o3}) and relative contribution (a_{o3}) of the longest open state were similar ($P > 0.05$, Table 2). The shortest and intermediate open states of mutant single-channel currents, however, had time constants (τ_{o1} and τ_{o2}) that were briefer than for wild-type receptor currents ($P < 0.001$, $P < 0.05$, Table 2). Moreover, there was a shift in the relative contributions of both brief open states (a_{o1} and a_{o2}) for mutant single-channel currents that was due to increased frequency of occurrence of the fastest component and reduced frequency of occurrence of the slowest component (Fig. 7*G* right panel) ($P < 0.001$, $P < 0.01$, Table 2). Thus, mutant single-channel currents had significantly reduced mean open time relative to that of wild-type α6β2δ currents ($P < 0.05$, Table 2, Fig. 7*I*), and their opening frequency was only about one-third of wild-type channel opening frequency ($P < 0.01$, Table 2, Fig. 7*J*). In contrast, there was no alteration of the main conductance state of mutant channels (~25 pS) when compared to wild-type channels (~26 pS) ($P > 0.05$, Table 2, Fig. 7*H*).

The α6 subunit mutation, R46W, decreased both burst duration and frequency of α6β2δ receptor currents

Both α6β2δ and α6(R46W)β2δ receptor channels opened in bursts (Fig. 8). Wild-type channels (Fig. 8*A*, top panel) opened with single brief openings and bursts of longer openings, while mutant channels opened with very

© 2011 The Authors. Journal compilation © 2011 The Physiological Society

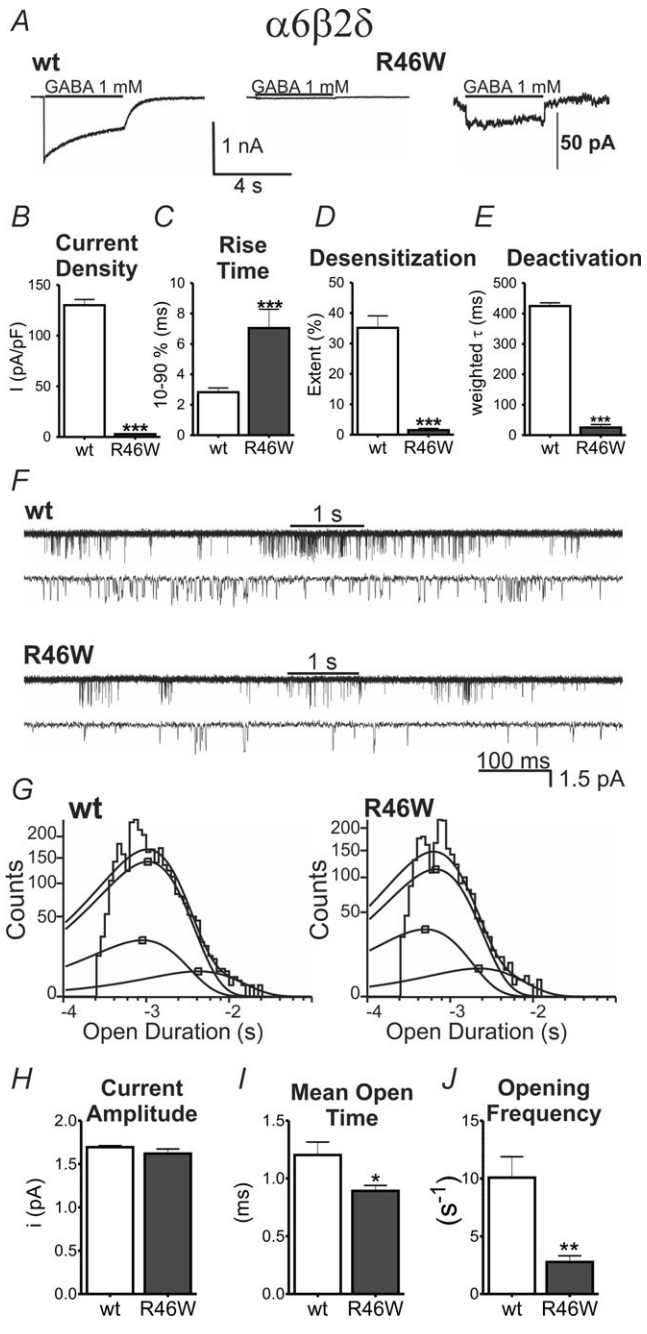

Figure 7. The R46W mutation had a greater effect on the function of $\alpha6\beta2\delta$ than on $\alpha6\beta2\gamma2$L receptors
A, current responses to long (4 s) applications of 1 mM GABA to lifted cells containing wild-type (wt) and mutant R46W $\alpha6\beta2\delta$ receptors are shown. Note that the right trace (1 nA bar scale) of the R46W current was expanded to the left (50 pA bar scale) to demonstrate the mutant current amplitude. *B–E*, current density, 10–90% rise time, desensitization extent and deactivation rate were measured during 4 s pulses of 1 mM GABA for both wild-type (white bars) and mutant (grey bars) receptors. *F*, steady-state single-channel currents were obtained from cell-attached patches containing wild-type (wt) and mutant R46W $\alpha6\beta2\delta$ receptors. Patches were voltage clamped at +80 mV and continuously exposed to 1 mM GABA. Note that the upper traces (1 s, black bars) were expanded below them. *G*, representative open duration histograms were plotted for both wild-type and mutant R46W $\alpha6\beta2\delta$ receptors and were fitted to three exponential functions. *H–J*, current amplitude (*H*), mean open time (*I*) and opening frequency (*J*) for both wild-type (white bars) and mutant R46W (grey bars) $\alpha6\beta2\delta$ receptors are shown. Values represent mean ± SEM. Differences between wild-type and mutant channels are shown as *, ** and ***, which indicate $P < 0.05$, $P < 0.01$ and $P < 0.001$ (unpaired *t* test).

brief openings (Fig. 8*A*, bottom panel). Since a major determinant of burst structure is the time constants of the two shortest closed states that occur within bursts (τ_{c1} and τ_{c2}), we compared the frequency of occurrence of these intraburst closures between wild-type and mutant receptor channels. Mutant receptors had shorter intraburst closures than wild-type receptors ($P < 0.05$, Table 2), but no differences were found in the relative occurrence (a_{c1} and a_{c2}) of these closures ($P > 0.05$, Table 2). Interestingly, the overall relative contribution of intraburst closures for both wild-type and mutant δ subunit-containing receptors were only 1/3 of the wild-type and mutant γ2L subunit-containing receptors (Table 2). This is consistent with the propensity of $\alpha6\beta2\delta$ receptors to open in bursts of brief openings, and for $\alpha6\beta2\gamma2$L receptors to open in clusters of bursts (Saxena & Macdonald, 1994; Fisher & Macdonald, 1997).

Consistent with the shorter mean open duration, $\alpha6$(R46W)$\beta2\delta$ channel burst durations were reduced when compared to wild-type channels ($P < 0.001$, Table 2, Fig. 8*C*). In addition, the time that $\alpha6$(R46W)$\beta2\delta$ channels spent within the burst (P_o) was much less than that of control channels ($P < 0.01$, Table 2, Fig. 8*B*), and the burst frequency of mutant channels was also less than that of wild-type channels ($P < 0.05$, Table 2, Fig. 8*D*). Furthermore, mutant channels had a small reduction of the number of openings per burst compared to wild-type channels ($P > 0.05$, Table 2).

Similar to γ2L subunit-containing $GABA_A$ receptors, for both wild-type $\alpha6\beta2\delta$ and mutant $\alpha6$(R46W)$\beta2\delta$ channels, the burst duration frequency distributions were fitted best by two exponential functions (Fig. 8*E*). Again, there were no differences in the time constants (τ_1 and τ_2) for the short-duration bursts (τ_1) for wild-type and mutant channels ($P > 0.05$, Table 2, Fig. 8*F*, left panel), and the time constant for the longer burst component (τ_2) was reduced for the mutant channel ($P < 0.05$, Table 2, Fig. 8*F*, right panel). Again, mutant receptors shifted the distribution of the two populations of burst durations by increasing the relative proportion of bursts with short duration (a_1) and reducing the relative proportion of longer bursts (a_2) ($P < 0.001$, Table 2, Fig. 8*G*). In summary, the $\alpha6$ subunit mutation, R46W, substantially impaired the gating of $\alpha6\beta2\delta$ channels that resulted in reduced macroscopic currents and altered kinetic properties.

© 2011 The Authors. Journal compilation © 2011 The Physiological Society

The α6 subunit mutation, R46W, decreased surface expression of $\alpha6\beta2\delta$ receptors

As described previously, both macroscopic and microscopic kinetic properties of $\alpha6\beta2\delta$ receptors were impaired by the α6(R46W) subunit mutation. Primarily we found a substantial reduction in α6(R46W)$\beta2\delta$ current density, which was due in part to the mutation's effect of reducing mean channel open time but could also be due to reduced expression of $\alpha\beta\delta$ receptors on the cell surface. To determine how expression of mutant α6(R46W) subunits affected expression of $\alpha6\beta2\delta$ receptors, homozygous wild-type $\alpha6^{FLAG}$ or mutant α6(R46W)^{FLAG} subunits were coexpressed with $\beta2$ and δ^{HA} subunits in HEK 293T cells, and surface and total cell expression levels of each subunit ($\alpha6^{FLAG}$, α6(R46W)^{FLAG}, $\beta2$ and $\gamma2L^{HA}$) were assessed using flow cytometry.

In contrast to the results obtained for $\alpha6\beta2\gamma2$L receptors, coexpression of α6(R46W)^{FLAG} with $\beta2$ and δ^{HA} subunits resulted in a general reduction of $\alpha6$, $\beta2$ and δ subunits on the cell surface (Fig. 9*A*). Cell surface levels of α6(R46W)^{FLAG} (0.63 ± 0.03, $n = 9$), $\beta2$ (0.72 ± 0.02, $n = 10$) and δ^{HA} (0.59 ± 0.01, $n = 10$) subunit levels were all lower ($P < 0.001$) than those determined for coexpression of wild-type $\alpha6^{FLAG}$ with $\beta2$ and δ^{HA} subunits ($\alpha6^{FLAG}$, 0.997 ± 0.001, $n = 9$; $\beta2$, 0.99 ± 0.001, $n = 10$; δ^{HA}, 1.00 ± 0.001, $n = 10$) (Fig. 9*B*). Moreover, total expression of α6(R46W)^{FLAG} subunits (0.44 ± 0.03, $n = 10$, $P < 0.001$, Fig. 9*C* and *D*, left panels) was half that of wild-type $\alpha6^{FLAG}$ subunits (0.999 ± 0.001, $n = 10$). This reduction was associated with a reduction of δ^{HA} subunit total levels (0.81 ± 0.05, $n = 10$, and 0.99 ± 0.001, $n = 10$, respectively, $P < 0.01$, Fig. 9*C* and *D*, right panels) but no changes in coexpressed $\beta2$ subunits (0.96 ± 0.09, $n = 7$, and 0.997 ± 0.001, $n = 10$, respectively, $P > 0.05$, Fig. 9*C* and *D*, middle panels). In summary, the R46W mutation caused a major reduction of surface expression of all subunits in $\alpha\beta\delta$ receptors.

Heterozygous coexpression of $\alpha6^{FLAG}/\alpha$6(R46W) with $\beta2$ and δ^{HA} subunits resulted in no significant difference in $\alpha6$ subunits (0.64 ± 0.02, $n = 7$, $P > 0.05$), and a small reduction of $\beta2$ (0.85 ± 0.03, $n = 8$, $P < 0.05$) and δ^{HA} (0.78 ± 0.02, $n = 8$, $P < 0.001$) subunits (Fig. 9*E*, top panels) on the cell surface, when compared to half-tagged $\alpha6^{FLAG}/\alpha6$ subunits (0.61 ± 0.02, $n = 7$, 1.01 ± 0.04, $n = 7$, and 0.99 ± 0.04, $n = 7$, respectively, dotted lines). Coexpression of $\alpha6/\alpha$6(R46W)^{FLAG} subunits, however, resulted in a larger reduction of $\alpha6$ subunits (0.28 ± 0.03, $n = 7$) relative to both half-tagged ($P < 0.001$) and heterozygous $\alpha6^{FLAG}/\alpha$6(R46W) ($P < 0.001$) receptors on the cell surface (Fig. 9*E*, left top panel) and was associated with a reduction of $\beta2$ (0.83 ± 0.04, $n = 8$, $P < 0.01$) and δ^{HA} (0.72 ± 0.03, $n = 8$, $P < 0.001$) subunit surface levels relative to half-tagged wild-type subunits, respectively (Fig. 9*E*, middle and right top panels).

When full-tagged $\alpha6^{FLAG}/\alpha$6(R46W)^{FLAG} subunits were coexpressed, $\alpha6$ subunit levels were increased on the cell surface (0.84 ± 0.02, $n = 6$) when compared to those obtained with $\alpha6/\alpha$6(R46W)^{FLAG} subunit coexpression ($P < 0.001$), and were slightly increased compared to FLAG levels with both

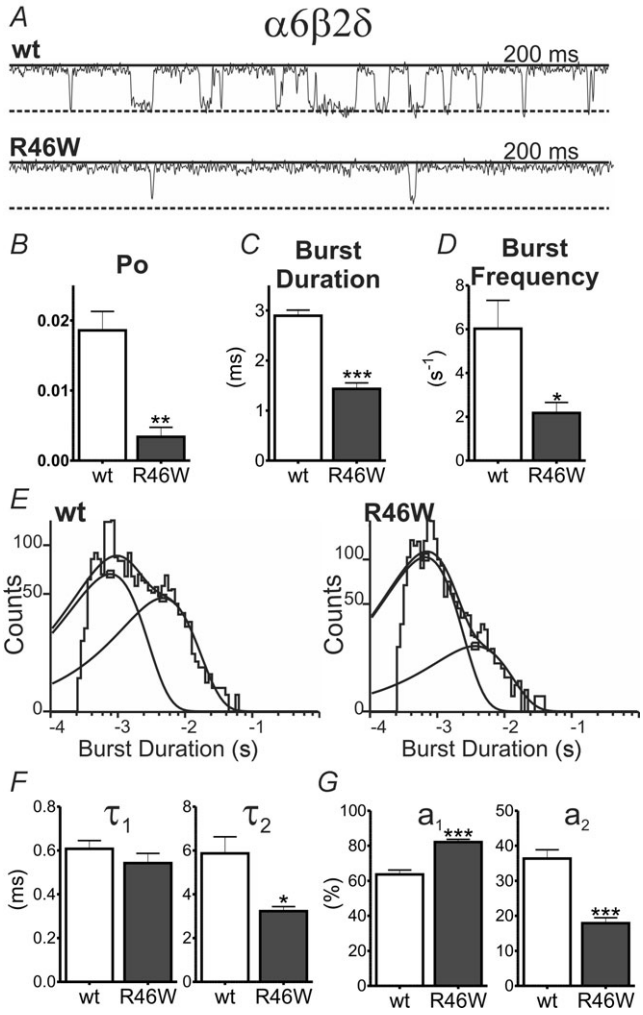

Figure 8. The R46W mutation decreased both burst duration and frequency of $\alpha6\beta2\delta$ receptor currents
A, representative steady-state single-channel burst traces from cell-attached patches containing wild-type (wt) and mutant R46W $\alpha6\beta2\delta$ receptors are presented. Patches were voltage clamped at +80 mV and continuously exposed to 1 mM GABA. *B–D*, comparisons of burst kinetics for both wild-type (white bars) and mutant R46W (grey bars) receptors are shown. *E*, representative burst duration histograms for both wild-type and mutant R46W $\alpha6\beta2\delta$ receptors were fitted to two exponential functions. *F* and *G*, time constants (τ) and representative areas (*a*) of burst duration histograms for both wild-type (white bars) and mutant R46W receptors (grey bars) are presented. Values represent mean ± SEM. Differences between wild-type and mutant channels are shown as *, ** and ***, which indicate $P < 0.05$, $P < 0.01$ and $P < 0.001$ (unpaired *t* test).

© 2011 The Authors. Journal compilation © 2011 The Physiological Society

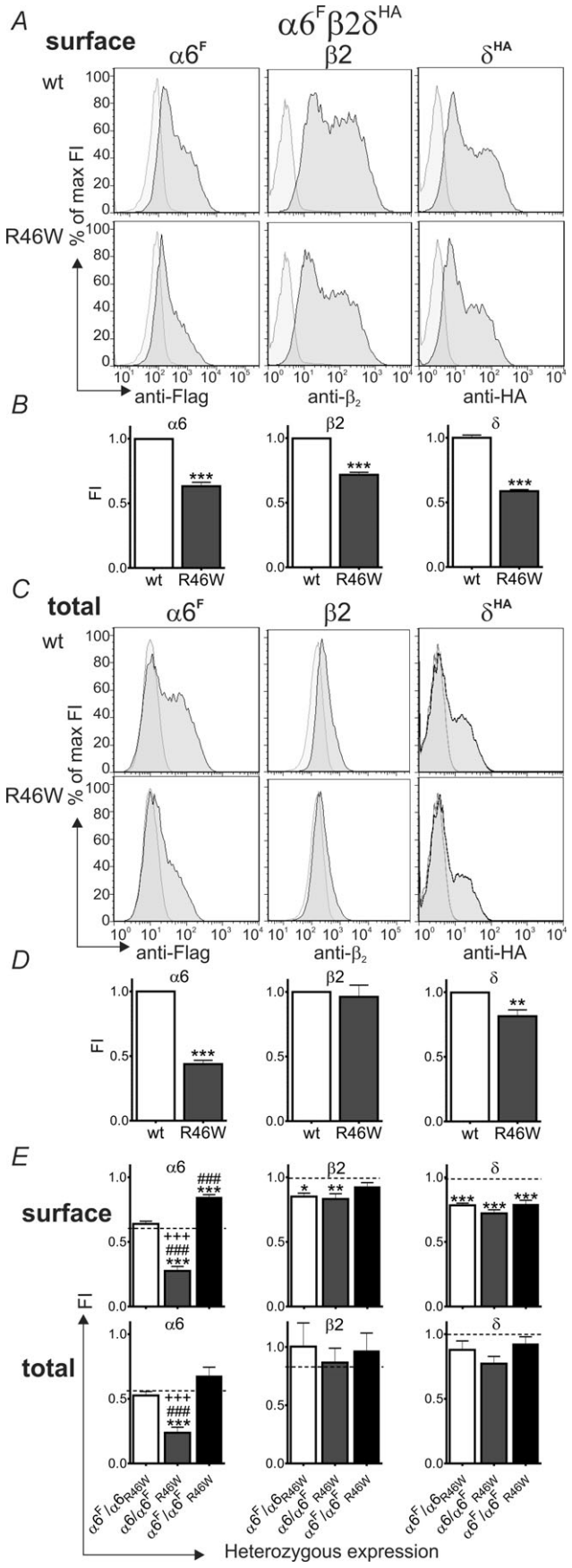

half-tagged $\alpha6^{FLAG}/\alpha6$ ($P < 0.001$) and heterozygous $\alpha6^{FLAG}/\alpha6$(R46W) ($P < 0.001$) expression (Fig. 9*E*, left top panel). No differences were found in surface expression levels of $\beta2$ subunits (0.93 ± 0.03, $n = 6$, $P > 0.05$) coexpressed with $\alpha6^{FLAG}/\alpha6(R46W)^{FLAG}$ subunits (Fig. 9*E*, right middle panel), but a reduction in surface levels of δ^{HA} subunits (0.79 ± 0.03, $n = 6$, $P < 0.001$) was found when compared to the half-tagged condition (Fig. 9*E*, right top panel). As with $\alpha\beta\gamma$ receptors, these results suggested that in heterozygous $\alpha6/\alpha6(R46W)\beta\delta$ receptors, mutant subunits were incorporated into the surface-trafficked receptors less efficiently than wild-type subunits. Specifically, in heterozygous $\alpha6/\alpha6(R46W)\beta\delta$ receptors, about 2/3 of all surface $\alpha6$ subunits were wild-type and 1/3 were mutant (Fig. 9*E* left top panel).

We also measured the total cellular expression of heterozygous $\alpha6/\alpha6(R46W)\beta2\delta^{HA}$ receptors (Fig. 9*E*, bottom panels). Similar to the results obtained for heterozygous expression of $\alpha6^{FLAG}/\alpha6(R46W)\beta2\gamma2L^{HA}$ receptors, no differences were found in total expression of $\alpha6$ (0.53 ± 0.03, $n = 7$, $P > 0.05$), $\beta2$ (1.00 ± 0.20, $n = 5$, $P > 0.05$) or δ^{HA} (0.88 ± 0.07, $n = 8$, $P > 0.05$) subunits when compared to half-tagged $\alpha6^{FLAG}/\alpha6$ subunit total expression (0.56 ± 0.03, $n = 7$; 0.83 ± 0.05, $n = 4$; and 1.00 ± 0.04, $n = 7$; respectively, dotted lines),

Figure 9. The R46W mutation decreased surface expression of all subunits in $\alpha\beta\delta$-containing receptors
A, $GABA_A$ receptor $\alpha6^F$, $\alpha6^F$(R46W), $\beta2$ and δ^{HA} subunit surface levels were measured by flow cytometry for cells coexpressing wild-type (wt) and mutant R46W $\alpha6\beta2\delta$ receptors. Representative histograms of positively transfected cells (dark grey) were superimposed on those from mock transfected cells (light grey) and are shown for surface expression. Note that the abscissa is a log scale. *B*, mean fluorescence intensity (FI) of $\alpha6$, $\beta2$ and δ subunit surface levels was quantified for both wild-type (white bars) and mutant receptors (grey bars). *C*, $GABA_A$ receptor $\alpha6^F$, $\alpha6^F$(R46W), $\beta2$ and δ^{HA} subunit total cellular expression levels were measured by flow cytometry for cells coexpressing wild-type and mutant R46W $\alpha6\beta2\delta$ receptors. Representative histograms of positively transfected cells (dark grey) were superimposed on those from mock transfected cells (light grey). *D*, mean fluorescence intensity (FI) of $\alpha6^F$, $\beta2$ and δ^{HA} subunit total levels was quantified as described above (wild-type as white bars, and mutant receptors as grey bars). Differences between wild-type and mutant channels are shown as ** and ***, which indicate $P < 0.01$ and $P < 0.001$ (unpaired *t* test). *E*, mean fluorescence intensity (FI) of $\alpha6^F$, $\beta2$ and δ^{HA} subunit surface and total expression was quantified for heterozygous $\alpha6^F/\alpha6$(R46W), $\alpha6/\alpha6(R46W)^F$ and $\alpha6^F/\alpha6(R46W)^F$ $\alpha6\beta2\delta$ receptor. Dashed lines represent $\alpha6^F/\alpha6$ surface or total levels. Values represent mean ± SEM. *, ** and *** indicate $P < 0.05$, $P < 0.01$ and $P < 0.001$ (one-way ANOVA) statistically different from wild-type ($\alpha6$ or $\alpha6^F/\alpha6$, see text for details), respectively. ## and ### indicate $P < 0.01$ and $P < 0.001$ (one-way ANOVA) statistically different from $\alpha6$(R46W) or $\alpha6^F/\alpha6$R46W. +++ indicates $P < 0.001$ (one-way ANOVA) statistically different from $\alpha6/\alpha6R46W^F$. ^{F}, FLAG.

© 2011 The Authors. Journal compilation © 2011 The Physiological Society

and no significant differences were found in total expression levels of β2 (0.87 ± 0.12, $n = 5$ and 0.96 ± 0.15, $n = 3$) or δ (0.77 ± 0.06, $n = 8$, and 0.92 ± 0.06, $n = 6$) subunits with heterozygous coexpression with either α6/α6(R46W)^{FLAG} or α6^{FLAG}/α6(R46W)^{FLAG} subunits, respectively (Fig. 9*E*, middle and right bottom panels). Coexpression of α6/α6(R46W)^{FLAG} subunits, however, resulted in a lower levels of total α6 subunits (0.24 ± 0.04, $n = 8$) than of either half-tagged α6^{FLAG}/α6 ($P < 0.001$) or heterozygous α6^{FLAG}/α6(R46W) ($P < 0.001$) subunits (Fig. 9*E*, left bottom panel). Moreover, when full-tagged α6^{FLAG}/α6(R46W)^{FLAG} subunits were coexpressed, there was an increase of total FLAG levels (0.68 ± 0.07, $n = 6$) when compared to FLAG levels with α6/α6(R46W)^{FLAG} coexpression ($P < 0.001$). Similar results were observed for total expression of α6 subunits (wild-type α6 subunits ∼2/3 and mutant α6(R46W) subunits ∼1/3) in α6/α6(R46W)β2γ2L-containing receptors (Figs 6*D* and 9*E*, left bottom panels).

Discussion

We determined the functional consequences of the $GABA_A$ receptor α6 subunit missense mutation, R46W, found in a patient with childhood absence epilepsy (CAE) and atonic seizures (Dibbens *et al.* 2009). The mutation is located in the N-terminus of the α6 subunit in a region homologous to a γ2 missense mutation, R82Q, that was reported in affected individuals having both CAE and febrile seizures (Wallace *et al.* 2001; Marini *et al.* 2003). The γ2 subunit mutation, R82Q, reduced current amplitude without altering current time course by impairing primarily receptor trafficking, thus reducing receptor surface expression (Bianchi *et al.* 2002*b*; Kang & Macdonald, 2004). In contrast we found that the α6 subunit mutation, R46W, linked to human CAE affected both gating properties and trafficking of human α6β2γ2 and α6β2δ receptors.

The α6 subunit mutation, R46W, impaired gating of α6β2γ2 and α6β2δ receptors

While the α6(R46W) subunit mutation reduced the current density of γ2 subunit-containing $GABA_A$ receptors by ∼25%, the mutation reduced the current density of δ subunit-containing receptors by 98% when compared with wild-type receptors. In addition to having reduced current amplitude, α6(R46W)β2γ2 currents displayed more macroscopic desensitization and slower deactivation kinetics. In contrast, α6(R46W)β2δ currents did not desensitize and deactivated rapidly. The mutation slowed activation rates of both α6β2γ2 and α6β2δ currents to a similar extent. The mutation also produced similar changes in the single-channel properties of α6β2γ2 and α6β2δ receptors, reducing both mean open time and burst duration. A reduction in current density could be produced by reduction of channel density on the cell surface (an issue discussed later) and/or by reduction of the time the channel spends in the open state. As a result, inhibitory postsynaptic current (IPSC) amplitudes would be reduced, potentially causing disinhibition and development of epilepsy. Reduced $GABA_A$ receptor function with mutations linked to CAE was also described with mutations of γ2(R82Q) and β3(G32R) $GABA_A$ receptor subunits (Bianchi *et al.* 2002*b*; Tanaka *et al.* 2008; Goldschen-Ohm *et al.* 2010). All of these mutations are located in the N-terminal extracellular subunit domain including the α-helix and before the first β-sheet. Within this domain, the γ2(R82Q) mutation is predicted to be located at the γ(+)/β(−) subunit interface, and the β3(G32R) subunit mutation is predicted to be located at the γ(+)/β(−) and α(+)/β(−) subunit interfaces in assembled receptors. In HEK 293 cells, Bianchi *et al.* (2002*a*) found that α1β3γ2(R82Q) receptors had reduced macroscopic peak currents and single-channel mean open duration, and Tanaka *et al.* (2008) reported that α1β3(G32R)γ2 receptors had reduced current density. Goldschen-Ohm *et al.* (2010) reported that $GABA_A$ receptors containing the γ2(R82Q) mutation had slowed deactivation by slowing recovery from desensitization and GABA unbinding, but without changes in the conductance of the channel. We conclude that both of these mutations affect channel function through structural conformational changes in the extracellular domain that links to channel gating and desensitization–deactivation coupling, thus probably altering the amplitude and duration of IPSCs.

Once GABA binds to $GABA_A$ receptors, rearrangements at the binding site trigger transitions among open, closed and desensitized states, which couples gating, desensitization and deactivation (Jones & Westbrook, 1995; Bianchi *et al.* 2001, 2002*a*; Bianchi & Macdonald, 2002). Our results demonstrate that the R46W mutation affects gating efficacy and desensitization–deactivation coupling of both γ and δ subunit-containing $GABA_A$ receptors. For γ subunit-containing receptors, gating efficacy was decreased by reducing burst duration, which makes the channel open in brief bursts that apparently prolonged channel deactivation. It seems that desensitization is coupled to deactivation in γ subunit-containing $GABA_A$ receptors. In contrast, with δ subunit-containing $GABA_A$ receptors, the smaller opening/burst frequencies predict faster deactivation of the channel. The effect of the mutation on the macroscopic desensitization and deactivation of the channel is governed by the subunit that completes the pentameric receptor. This is important since γ (synaptic) and δ (extrasynaptic) subunit-containing $GABA_A$ receptors confer different properties to the synapse.

© 2011 The Authors. Journal compilation © 2011 The Physiological Society

The α6(R46W) subunit mutation impaired assembly or/trafficking of both α6β2γ2 and α6β2δ receptors

Multiple motifs for efficient subunit folding and receptor assembly have been described in the N-terminal extracellular domains of $GABA_A$ receptor subunits (Tretter *et al.* 1997; Taylor *et al.* 1999, 2000; Klausberger *et al.* 2000). These motifs are structurally conserved among $GABA_A$ receptor subunits and involve intermolecular binding interactions between side chains of residues located on subunit interfaces. The α6(R46W) mutation is located at the α(+) interface of $GABA_A$ receptors. Thus, this mutation could impair oligomerization at the α(+)/γ(−), α(+)/δ(−) and α(+)/β(−) subunit interfaces, potentially impairing assembly or altering the stoichiometry of receptors.

The α1(+) subunit interface was reported to interact with a group of residues at the γ2(−) subunit interface that are homologous to residues at the (−) interface of β subunits where the missense mutation γ2(R82Q) disrupts a highly conserved inter-subunit contact site (Klausberger *et al.* 2000; Hales *et al.* 2005). Hales and colleagues suggested that the mutant γ2(R82Q) subunit has impaired oligomerization at the γ2(+)/β2(−) subunit interface during receptor assembly (Hales *et al.* 2005). This failure of assembly and folding of mutant γ2(R82Q) subunits result in retention of the mutant subunit in the endoplasmic reticulum (ER) and reduction of surface expression levels of α1β2γ2 receptors (Kang & Macdonald, 2004; Sancar & Czajkowski, 2004). We found that coexpression of mutant α6(R46W) subunits decreased surface expression levels of all partnering subunits in αβδ receptors, and α and β subunits in αβγ receptors, suggesting misfolding of excess subunits and later ER retention and degradation (Kang & Macdonald, 2004). It was proposed that non-degraded or residual mutant $GABA_A$ receptor α1(A322D) subunits linked to juvenile myoclonic epilepsy produced a dominant negative effect by association and retention of wild-type receptor subunits (Ding *et al.* 2010). However, heterozygous coexpression of mutant α6(R46W) and wild-type α6 subunits restored ∼68% of the macroscopic current amplitude by expressing more wild-type than mutant subunits and assembling α6/α6(R46W)β2γ2L receptors on the cell surface. Thus, mutant α6(R46W) subunits can access the cell surface and form $GABA_A$ receptors with different subunit arrangements. Although the presumed stoichiometry of ternary $GABA_A$ receptors is 2α, 2β and 1γ/δ subunits (Tretter *et al.* 1997), the assembly and trafficking of other subunits to the cell surface is restricted to a limited number of receptor stoichiometries (Angelotti & Macdonald, 1993; Connolly *et al.* 1996; Taylor *et al.* 2000). Using concatenated subunits it was suggested that the α1(A322D) subunit mutation, which impaired these interactions, produced asymmetrical subunit composition of functional heteromeric $GABA_A$ receptors on the cell surface (Gallagher *et al.* 2004). It seems that the α6(R46W) subunit mutation could also impair intersubunit binding interactions differently at the α6β2 and α6γ2/δ interfaces, differently affecting the subunit arrangement of $GABA_A$ receptors expressed on the cell surface.

Mutation of R46 in the α-helix loop 1 zone weakens interactions at the interfaces of γ2, δ and β2 subunits and alters channel function through structural conformational changes in the extracellular domain that mediate links to channel gating and desensitization

Structural studies showed a common mechanism for translating ligand binding to channel gating for Cys-loop ligand ion channels (Mukhtasimova *et al.* 2005; Unwin, 2005; Sine & Engel, 2006; Gay & Yakel, 2007). These included conformational rearrangements of the C-loop within the ligand-binding pocket followed by movements of loops 2 and 7 (Cys-loop) where critical residues interact upon agonist binding. These conformational rearrangements in the binding zone are transmitted to the coupling zone through interactions between the β1–β2 loop and the M2–M3 linker, which propagate structural movements from the binding site to the transmembrane domains allowing channel opening. It is possible that the R46W mutation in the α helix–loop 1 zone of the α6 subunit weakens the interactions at the interfaces of γ2, δ and β2 subunits, propagating allosteric conformational changes through the rigid β-strands, causing rearrangements within the coupling zone of α6β2γ2/δ receptors. Thus this mutation could affect channel function through structural conformational changes in the extracellular domain that links to channel gating and desensitization. It was proposed that the missense mutation γ2(R82Q) eliminates benzodiazepine binding to the putative benzodiazepine-binding site at the γ/β interface (Cromer *et al.* 2002), which is on the opposite side of the γ subunit (γ2(−)), through allosteric conformational change of a salt-bridge network existing between this arginine and charged residues at the γ2(+)/β2(−) interface of α1β2γ2 $GABA_A$ receptors. Charge reversal or neutralization of the residues positioned in this salt-bridge network impaired $GABA_A$ receptor macroscopic kinetics and diazepam sensitivity of α1β2γ2 receptors expressed in HEK 293 cells (Goldschen-Ohm *et al.* 2010). At the homologous position of α6R46, a comparative structural model of the extracellular domain of α1β2γ2 receptors based on homology with the crystal structure of the nACh receptor (Ernst *et al.* 2005; Unwin, 2005) suggested that the arginine (α1R29) shares bonding interactions between the side chains of acidic (β2D89, α1D27) and

© 2011 The Authors. Journal compilation © 2011 The Physiological Society

amide (α1N28, γ2N101) residues at the interfaces of β2(–) and γ2(–) subunits that stabilizes the tertiary structure of the subunits. These residues were identified as a part of a conserved assembly motif in α1 subunits (Klausberger *et al.* 2000). Homology modelling of the N-terminal extracellular domain of $\alpha6\beta2\gamma2$ and $\alpha6\beta2\delta$ receptors shows a lack (α6D44, γ2N71, β2D41, β2D113 and δD45) of interactions between the side chains in the interfaces of α6(+) and β2(–), γ2(–), or δ(–) subunits when the α6 subunit R46 is mutated to W46 (Fig. 10), which might first change the surface accessible area of the residues between the interfaces of the subunits, and second propagate intramolecular and/or intermolecular allosteric conformational changes through the rigid β-strands, causing rearrangements within the coupling zone of $GABA_A$ receptors. Moreover, when an agonist binds to these receptors, conformational changes trigger the 'capping motion' of the C-loop in toward the channel over the agonist, which couples agonist binding to channel gating (Mukhtasimova *et al.* 2005; Sine & Engel, 2006). A similar mechanism was proposed to occur at the homologous structural region of the C-loop of $\alpha1\beta2\gamma2$ $GABA_A$ receptors (Venkatachalan & Czajkowski, 2008). Hence electrostatic interactions between charged residues

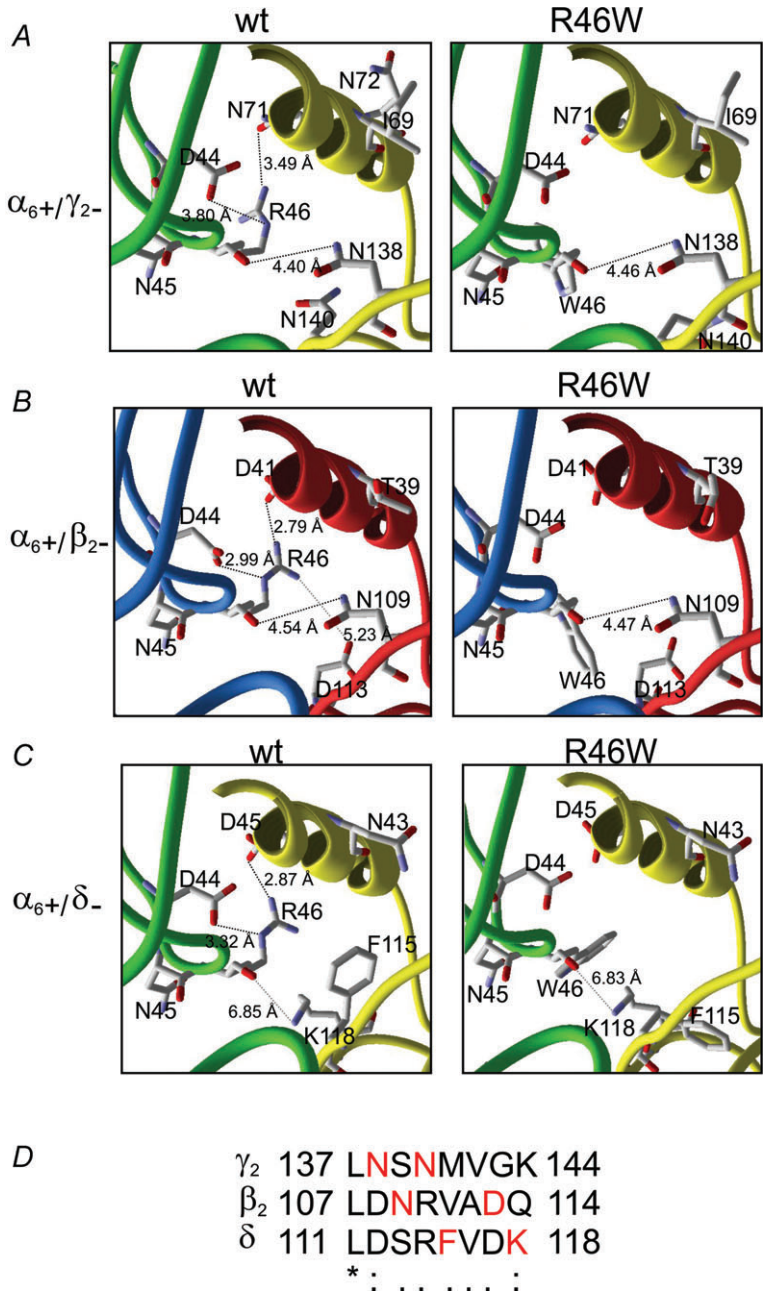

Figure 10. Mutation of α6R46 in the α-helix–loop-1 zone weakens interactions at the interfaces of γ2, β2 and δ subunits
A–C, close view of the α-helix–loop-1 zone of the structural modelling of the $GABA_A$ receptor at the interface between α6(+) and γ2(–), β2(–) and δ(–) subunits showing the predicted interactions (<4.60 Å, black dotted lines; and >4.60 Å, grey dotted lines) between side chains of α6R46 (wt, left panels) and α6W46 (R46W, right panels). Note that γ2N71, β2D41 and δD45 are conserved residues into the α-helix across the GABAR subunits (see Fig. 1*B*). The backbones of subunits are represented as coloured ribbons as showed in Fig. 1*A* (α6 in green and blue, β2 in red, and γ2 and δ in yellow) and labelled residues as CPK colour representation. *D*, sequence alignment of the putative homologous assembly motif at human γ2(–), β2(–) and δ(–) subunit interfaces is presented. Predicted residues at the interfaces are in red. '*', ':' and '.' mean that residues are identical, conserved or semi-conserved in all sequences in the alignment.

© 2011 The Authors. Journal compilation © 2011 The Physiological Society

of loop-B and loop-C might be involved in the C-loop mobility during activation of $GABA_A$ receptors and could be affected by structural changes transmitted through the β-strands by either modification of glycosylation sites (Lo *et al.* 2010) or by nearby point mutations located at the top of the N-terminal extracellular domain of the receptor as suggested for the missense mutation γ2(R82Q) (Goldschen-Ohm *et al.* 2010) and the α6(R46W) mutation (this study).

Pathophysiological consequences of $GABA_A$ receptor α6 subunit (*GABRA6*) mutations in CAE

It may be assumed that in pathological conditions, all neural networks are susceptible to amplification or intensification of aberrant signals from disinhibited neuronal networks. However, the functional consequences of these networks for epileptogenesis in the cerebellum are unclear. Early work (Homanics *et al.* 1997; Jones *et al.* 1997) failed to demonstrate any behavioural phenotype in mice lacking $GABA_A$ receptor α6 subunits; however, we cannot necessarily discount the possibility of the presence of absence seizures in these models since the detection of such events sometimes requires a phenotypic criterion such as abnormal EEG (generalized spike-wave discharges) rather than a simple observable behaviour. Nonetheless, the lack of α6 subunits caused a dramatic reduction in δ subunit protein levels in the cerebellum of α6 knockout mice (Jones *et al.* 1997). We found that the R46W mutation caused a similar reduction of surface expression of δ subunits, which unveils a critical role of this residue for proper assembling/trafficking of functional $GABA_A$ receptors. Likewise, a point mutation in a residue critical for benzodiazepine binding to α6 subunits (R100) conferred diazepam-mediated potentiation of α6(Q100)β2γ2 GABA-activated currents and reduced the impairment of postural reflexes produced by benzodiazepine agonists such as diazepam in alcohol non-tolerant rats (Korpi & Seeburg, 1993; Hanchar *et al.* 2005). We suggest that the R46W mutation may increase susceptibility to epilepsy syndromes such as CAE through a reduction of $\alpha6\beta\gamma$ and $\alpha6\beta\delta$ receptor function and expression in the cerebellum. However, it is unclear whether or not, and if so how, the mutated α6 protein contributes to the pathogenesis of the epilepsy syndrome. Further validation of the mutant subunit *in vivo* will be required to determine whether this mutation contributes to shaping the disease phenotype.

References

Angelotti TP & Macdonald RL (1993). Assembly of $GABA_A$ receptor subunits: $\alpha_1\beta_1$ and $\alpha_1\beta_1\gamma_{2S}$ subunits produce unique ion channels with dissimilar single-channel properties. *J Neurosci* **13**, 1429–1440.

Bianchi MT, Haas KF & Macdonald RL (2001). Structural determinants of fast desensitization and desensitization-deactivation coupling in $GABA_A$ receptors. *J Neurosci* **21**, 1127–1136.

Bianchi MT, Haas KF & Macdonald RL (2002*a*). α1 and α6 subunits specify distinct desensitization, deactivation and neurosteroid modulation of $GABA_A$ receptors containing the δ subunit. *Neuropharmacology* **43**, 492–502.

Bianchi MT & Macdonald RL (2002). Slow phases of $GABA_A$ receptor desensitization: structural determinants and possible relevance for synaptic function. *J Physiol* **544**, 3–18.

Bianchi MT, Song L, Zhang H & Macdonald RL (2002*b*). Two different mechanisms of disinhibition produced by $GABA_A$ receptor mutations linked to epilepsy in humans. *J Neurosci* **22**, 5321–5327.

Brejc K, van Dijk WJ, Klaassen RV, Schuurmans M, van Der Oost J, Smit AB & Sixma TK (2001). Crystal structure of an ACh-binding protein reveals the ligand-binding domain of nicotinic receptors. *Nature* **411**, 269–276.

Connolly CN, Krishek BJ, McDonald BJ, Smart TG & Moss SJ (1996). Assembly and cell surface expression of heteromeric and homomeric γ-aminobutyric acid type A receptors. *J Biol Chem* **271**, 89–96.

Cromer BA, Morton CJ & Parker MW (2002). Anxiety over $GABA_A$ receptor structure relieved by AChBP. *Trends Biochem Sci* **27**, 280–287.

Dellisanti CD, Yao Y, Stroud JC, Wang ZZ & Chen L (2007). Crystal structure of the extracellular domain of nAChR α1 bound to α-bungarotoxin at 1.94 Å resolution. *Nat Neurosci* **10**, 953–962.

Dibbens LM, Harkin LA, Richards M, Hodgson BL, Clarke AL, Petrou S, Scheffer IE, Berkovic SF & Mulley JC (2009). The role of neuronal $GABA_A$ receptor subunit mutations in idiopathic generalized epilepsies. *Neurosci Lett* **453**, 162–165.

Ding L, Feng HJ, Macdonald RL, Botzolakis EJ, Hu N & Gallagher MJ (2010). $GABA_A$ receptor α1 subunit mutation A322D associated with autosomal dominant juvenile myoclonic epilepsy reduces the expression and alters the composition of wild type $GABA_A$ receptors. *J Biol Chem* **285**, 26390–26405.

Ernst M, Bruckner S, Boresch S & Sieghart W (2005). Comparative models of $GABA_A$ receptor extracellular and transmembrane domains: important insights in pharmacology and function. *Mol Pharmacol* **68**, 1291–1300.

Fisher JL & Macdonald RL (1997). Single channel properties of recombinant $GABA_A$ receptors containing γ2 or δ subtypes expressed with α1 and β3 subtypes in mouse L929 cells. *J Physiol* **505**, 283–297.

Gallagher MJ, Song L, Arain F & Macdonald RL (2004). The juvenile myoclonic epilepsy $GABA_A$ receptor α1 subunit mutation A322D produces asymmetrical, subunit position-dependent reduction of heterozygous receptor currents and α1 subunit protein expression. *J Neurosci* **24**, 5570–5578.

Gay EA & Yakel JL (2007). Gating of nicotinic ACh receptors; new insights into structural transitions triggered by agonist binding that induce channel opening. *J Physiol* **584**, 727–733.

Goldschen-Ohm MP, Wagner DA, Petrou S & Jones MV (2010). An epilepsy-related region in the $GABA_A$ receptor mediates long-distance effects on GABA and benzodiazepine binding sites. *Mol Pharmacol* **77**, 35–45.

© 2011 The Authors. Journal compilation © 2011 The Physiological Society

Haas KF & Macdonald RL (1999). $GABA_A$ receptor subunit γ2 and δ subtypes confer unique kinetic properties on recombinant $GABA_A$ receptor currents in mouse fibroblasts. *J Physiol* **514**, 27–45.

Hales TG, Tang H, Bollan KA, Johnson SJ, King DP, McDonald NA, Cheng A & Connolly CN (2005). The epilepsy mutation, γ2(R43Q) disrupts a highly conserved inter-subunit contact site, perturbing the biogenesis of $GABA_A$ receptors. *Mol Cell Neurosci* **29**, 120–127.

Hanchar HJ, Dodson PD, Olsen RW, Otis TS & Wallner M (2005). Alcohol-induced motor impairment caused by increased extrasynaptic $GABA_A$ receptor activity. *Nat Neurosci* **8**, 339–345.

Hirose S, Mitsudome A, Okada M & Kaneko S (2005). Genetics of idiopathic epilepsies. *Epilepsia* **46**, 38–43.

Homanics GE, Ferguson C, Quinlan JJ, Daggett J, Snyder K, Lagenaur C, Mi ZP, Wang XH, Grayson DR & Firestone LL (1997). Gene knockout of the α6 subunit of the α-aminobutyric acid type A receptor: lack of effect on responses to ethanol, pentobarbital, and general anesthetics. *Mol Pharmacol* **51**, 588–596.

Jones A, Korpi ER, McKernan RM, Pelz R, Nusser Z, Makela R, Mellor JR, Pollard S, Bahn S, Stephenson FA, Randall AD, Sieghart W, Somogyi P, Smith AJ & Wisden W (1997). Ligand-gated ion channel subunit partnerships: $GABA_A$ receptor α_6 subunit gene inactivation inhibits δ subunit expression. *J Neurosci* **17**, 1350–1362.

Jones MV & Westbrook GL (1995). Desensitized states prolong $GABA_A$ channel responses to brief agonist pulses. *Neuron* **15**, 181–191.

Kang JQ & Macdonald RL (2004). The $GABA_A$ receptor γ2 subunit R43Q mutation linked to childhood absence epilepsy and febrile seizures causes retention of $\alpha1\beta2\gamma2$S receptors in the endoplasmic reticulum. *J Neurosci* **24**, 8672–8677.

Klausberger T, Fuchs K, Mayer B, Ehya N & Sieghart W (2000). $GABA_A$ receptor assembly. Identification and structure of γ_2 sequences forming the intersubunit contacts with α_1 and β_3 subunits. *J Biol Chem* **275**, 8921–8928.

Korpi ER & Seeburg PH (1993). Natural mutation of $GABA_A$ receptor alpha 6 subunit alters benzodiazepine affinity but not allosteric GABA effects. *Eur J Pharmacol* **247**, 23–27.

Lo WY, Botzolakis EJ, Tang X & Macdonald RL (2008). A conserved Cys-loop receptor aspartate residue in the M3-M4 cytoplasmic loop is required for $GABA_A$ receptor assembly. *J Biol Chem* **283**, 29740–29752.

Lo WY, Lagrange AH, Hernandez CC, Harrison R, Dell A, Haslam SM, Sheehan JH & Macdonald RL (2010). Glycosylation of β2 subunits regulates $GABA_A$ receptor biogenesis and channel gating. *J Biol Chem* **285**, 31348–31361.

Macdonald RL, Kang JQ & Gallagher MJ (2010). Mutations in $GABA_A$ receptor subunits associated with genetic epilepsies. *J Physiol* **588**, 1861–1869.

Macdonald RL & Olsen RW (1994). $GABA_A$ receptor channels. *Annu Rev Neurosci* **17**, 569–602.

Marini C, Harkin LA, Wallace RH, Mulley JC, Scheffer IE & Berkovic SF (2003). Childhood absence epilepsy and febrile seizures: a family with a $GABA_A$ receptor mutation. *Brain* **126**, 230–240.

Miyazawa A, Fujiyoshi Y & Unwin N (2003). Structure and gating mechanism of the acetylcholine receptor pore. *Nature* **423**, 949–955.

Mukhtasimova N, Free C & Sine SM (2005). Initial coupling of binding to gating mediated by conserved residues in the muscle nicotinic receptor. *J Gen Physiol* **126**, 23–39.

Sancar F & Czajkowski C (2004). A $GABA_A$ receptor mutation linked to human epilepsy (γ_2R43Q) impairs cell surface expression of $\alpha\beta\gamma$ receptors. *J Biol Chem* **279**, 47034–47039.

Saxena NC & Macdonald RL (1994). Assembly of $GABA_A$ receptor subunits: role of the δ subunit. *J Neurosci* **14**, 7077–7086.

Saxena NC & Macdonald RL (1996). Properties of putative cerebellar gamma-aminobutyric acid A receptor isoforms. *Mol Pharmacol* **49**, 567–579.

Schwede T, Kopp J, Guex N & Peitsch MC (2003). SWISS-MODEL: An automated protein homology-modeling server. *Nucleic Acids Res* **31**, 3381–3385.

Sine SM & Engel AG (2006). Recent advances in Cys-loop receptor structure and function. *Nature* **440**, 448–455.

Tanaka M, Olsen RW, Medina MT, Schwartz E, Alonso ME, Duron RM, Castro-Ortega R, Martinez-Juarez IE, Pascual-Castroviejo I, Machado-Salas J, Silva R, Bailey JN, Bai D, Ochoa A, Jara-Prado A, Pineda G, Macdonald RL & Delgado-Escueta AV (2008). Hyperglycosylation and reduced GABA currents of mutated *GABRB3* polypeptide in remitting childhood absence epilepsy. *Am J Hum Genet* **82**, 1249–1261.

Tang X, Hernandez CC & Macdonald RL (2010). Modulation of spontaneous and GABA-evoked tonic $\alpha4\beta3\delta$ and $\alpha4\beta3\gamma2$L $GABA_A$ receptor currents by protein kinase A. *J Neurophysiol* **103**, 1007–1019.

Taylor PM, Connolly CN, Kittler JT, Gorrie GH, Hosie A, Smart TG & Moss SJ (2000). Identification of residues within $GABA_A$ receptor α subunits that mediate specific assembly with receptor β subunits. *J Neurosci* **20**, 1297–1306.

Taylor PM, Thomas P, Gorrie GH, Connolly CN, Smart TG & Moss SJ (1999). Identification of amino acid residues within $GABA_A$ receptor β subunits that mediate both homomeric and heteromeric receptor expression. *J Neurosci* **19**, 6360–6371.

Tretter V, Ehya N, Fuchs K & Sieghart W (1997). Stoichiometry and assembly of a recombinant $GABA_A$ receptor subtype. *J Neurosci* **17**, 2728–2737.

Twyman RE, Rogers CJ & Macdonald RL (1990). Intraburst kinetic properties of the $GABA_A$ receptor main conductance state of mouse spinal cord neurones in culture. *J Physiol* **423**, 193–220.

Unwin N (2005). Refined structure of the nicotinic acetylcholine receptor at 4Å resolution. *J Mol Biol* **346**, 967–989.

Venkatachalan SP & Czajkowski C (2008). A conserved salt bridge critical for $GABA_A$ receptor function and loop C dynamics. *Proc Natl Acad Sci U S A* **105**, 13604–13609.

Wallace RH, Marini C, Petrou S, Harkin LA, Bowser DN, Panchal RG, Williams DA, Sutherland GR, Mulley JC, Scheffer IE & Berkovic SF (2001). Mutant $GABA_A$ receptor γ2-subunit in childhood absence epilepsy and febrile seizures. *Nat Genet* **28**, 49–52.

© 2011 The Authors. Journal compilation © 2011 The Physiological Society

Author contributions

C.C.H. and R.L.M. designed the research; C.C.H. and K.N.G. performed research and analysed the data; N.H. contributed new reagents; C.C.H. and R.L.M. wrote the paper. All authors approved the manuscript for publication.

Acknowledgements

This work was supported by NIH grants R01 NS51590 and NS33300 to R.L.M.

© 2011 The Authors. Journal compilation © 2011 The Physiological Society